

Class-E power amplifier design for wireless power transfer

Authors: Peter B. Green

About this document

Scope and purpose

The purpose of this document is to provide a comprehensive guide to the design of a class-E RF power amplifier for magnetic resonance wireless charging based on the Air Fuel baseline system specification (BSS). The scope applies to all technical aspects that should be considered in the design process, including tuning of the resonant circuit, inductor design and impedance matching to the transmit coil. Simulations are presented as well as test results from the 16W single ended class-E evaluation board.

Intended audience

Power supply/charger design engineers, applications engineers, students.

Table of Contents

1	Introduction.....	3
2	Air Fuel resonant wireless charging overview	5
2.1	Basic principles.....	5
2.2	Resonant coupling	7
2.3	PTU specifications.....	12
3	Class-E power amplifier.....	13
3.1	Passive component selection	14
3.2	MOSFET selection.....	17
3.3	Operation under varying load conditions	21
4	Simulated performance.....	22
4.1	Power amplifier driving a resistive load	22
4.2	Complete system simulation	26
5	SE class-E evaluation board	31
5.1	Functional description	31
5.2	Schematic	33
5.3	Bill of materials.....	34
5.4	PCB layout	36
6	RF inductor design	37
6.1	Output inductor.....	37
6.2	Current transformer	38
7	Transmit coil	39
8	Test receivers.....	40
8.1	Resistive load board	40
8.2	Elliptical LED receiver board.....	41
8.3	Receiver load board	41
9	Test results	43
9.1	Resistive load board tests	43
9.2	LED load board tests	45

Introduction

9.3	Receiver load board tests.....	47
10	Conclusion	50

Introduction

1 Introduction

Up until recently the only charging method available for portable devices (PD) such as notebooks, tablets and smart phones has been by cable connection to an external charger/adapter connected to an AC power source. The introduction of non-radiative¹ wireless charging technologies can eliminate adapters and cables when used with new generations of PDs, which include built in power receiving units (PRU).

This enables one or more PDs to be placed on a charging pad incorporating a power transmission unit (PTU) from which power is transferred by coupling through an oscillating magnetic field. Received power is then rectified and regulated inside the device to charge its internal battery.

Many low power wireless charging systems rely on inductive coupling such as that in the Wireless Power Consortium Qi standard, which operates in the 100 to 205 kHz frequency range. However this requires tight coupling over very limited distance and specific placement of the receiver coil in relation to the transmit coil limited to a maximum power capability of 15 W.

More recently the Alliance for Wireless Power has introduced the “Rezence” standard. The A4WP has now merged with the Power Matters Alliance (PMA) another organization working on inductive wireless charging in the 201 to 315 kHz range, to form the Air Fuel Alliance. The wireless power transfer system baseline system specification (BSS) [1] describes resonant inductive coupling operating at multiples of 6.78 MHz. 6.78MHz (wavelength 44.25m) is the lowest frequency of the industrial, scientific and medical (ISM) bands reserved by international agreement for purposes other than telecommunications. This enables transmission of up to 70 W of power over significantly greater distances in the order of tens of milli-metres. Furthermore one or more receiving devices may be placed in any orientation, while still being able to achieve sufficient coupling to the power transmission source. Resonant inductive coupling is a technique first proposed by Nicola Tesla in the early 20th century, in which power is transferred through an oscillating magnetic field between tuned circuits of the same resonant frequency in the transmitter and receiver, which greatly increases energy transfer.

The Rezence standard utilizes bi-directional communication via Bluetooth between the PD and the wireless power transmitter to request and control the amount of electromagnetic field energy transmitted. The basic system architecture is shown in the figure below. This application note covers general topics relating to wireless charging based on the BSS including; the transmit and receive resonators, matching circuit and power amplifier². There are several different power amplifier topologies available including different variations of class D and class-E. The single ended class-E topology will be covered here.

¹ “Non-radiative” refers to near field charging systems where the distance is much lower than the wavelength.

² The term “power amplifier” will be used in this application note since it is widely used to describe the power converter used in wireless charging although it is not in fact an amplifier.

Introduction

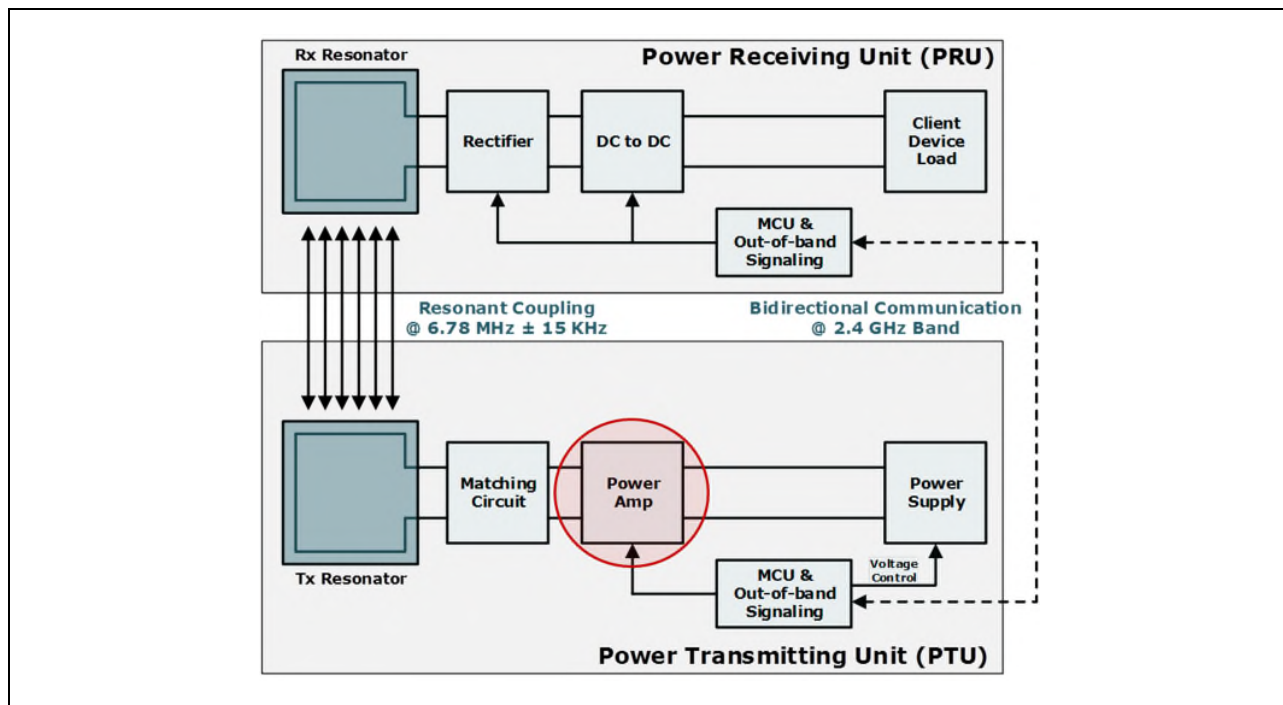


Figure 1 Wireless charging system overview

2 Air Fuel resonant wireless charging overview

2.1 Basic principles

An oscillating magnetic field (H-field) is produced by the current (I_{TX}) supplied to transmit (TX) coil from the PTU power amplifier, where the magnitude of I_{TX} should be between the coil minimum and maximum ratings I_{TX_MIN} and I_{TX_MAX} . The circular or rectangular spiral transmit coil lies flat to produce an approximately vertical H-field within the winding area and over a distance up to several 10s of millimetres.

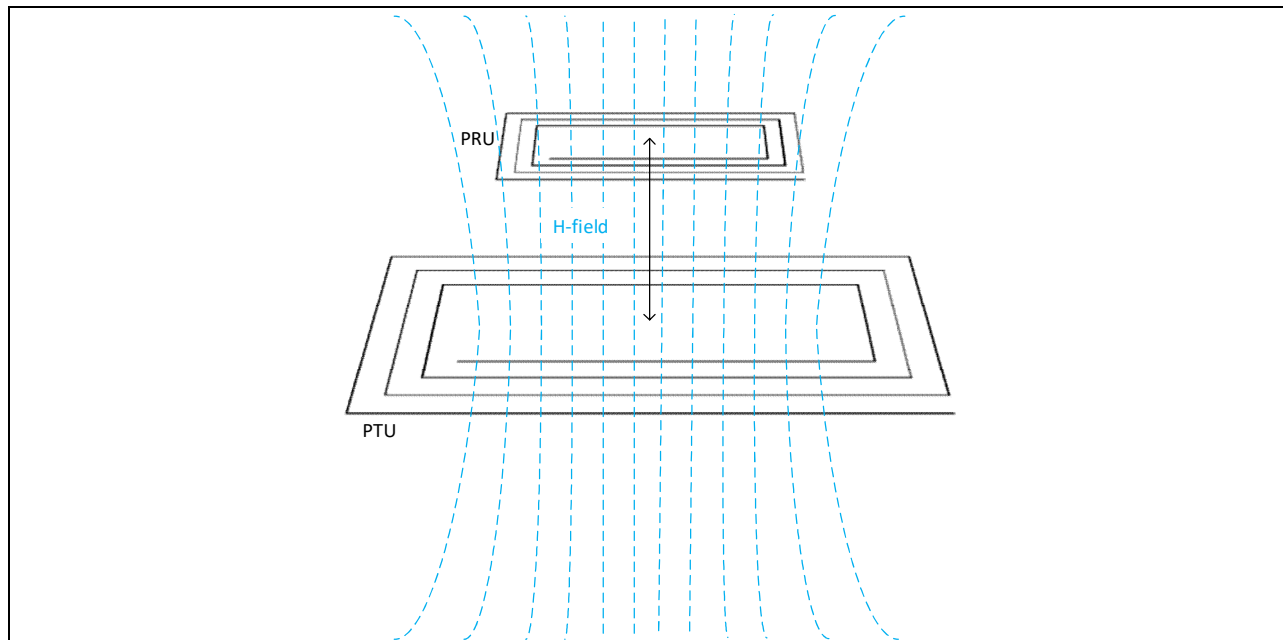


Figure 2 Magnetic field between PTU and PRU resonators

The wireless charging system based on the BSS operates by resonant coupling at 6.78MHz +/-15kHz. To accomplish this both the PTU and PRU must be tuned to this frequency. The transmit and receive coils when placed within range, behave as a transformer with a low coupling factor (k) inversely proportional to distance.

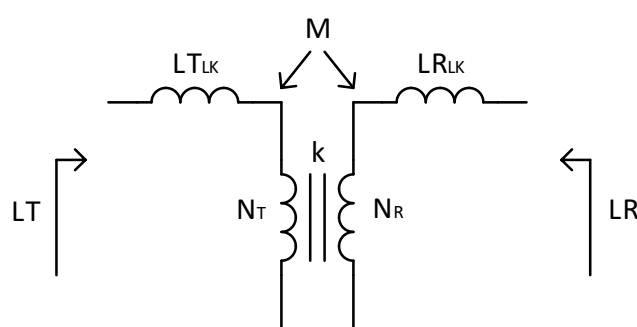


Figure 3 Transmit and receive coil coupling

Air Fuel resonant wireless charging overview

Tight coupling is defined as a coupling factor 'k' greater than 0.5. In wireless charging the coupling is loose with k typically less than 0.1. The mutual inductance between the two coils is given by:

$$M = \frac{\mu_0 \mu_r N_T N_R A_e}{l_e} \quad [H] \quad [1]$$

Where, N_T and N_R are the number of turns in each coil, typically 10 or less. A_e and l_e are the effective area and length of the magnetic path, which is dependent on the size, spacing and orientation of the coils relative to each other. μ_0 is the permeability of free space $4\pi \times 10^{-7}$ H/m and μ_r is the relative permeability of air, which is 1. The coupling factor k is related to the mutual inductance according to the formula:

$$k = \frac{M}{\sqrt{LT \cdot LR}} \quad \text{and} \quad M = k \cdot \sqrt{LT \cdot LR} \quad [2]$$

With a low k the leakage inductances LT_{LK} and LR_{LK} are large compared with the mutual inductance and magnetizing inductances of each coil:

$$LT_{LK} = LT - M \quad \text{and} \quad LR_{LK} = LR - M \quad [H] \quad [3]$$

To overcome the low coupling factor, the circulating currents in each side of the circuit are increased by operating at resonance to enable more efficient power transfer.

The BSS classifies power transmitting and receiving units according to their maximum power capabilities. These are summarized with device examples in the following tables:

Table 1 PRU Categories

PRU Category	Minimum Power Rating	Example Applications
Category 1	<2W	Bluetooth headset
Category 2	3.5W	Feature phone
Category 3	6.5W	Smart phone
Category 4	13W	Tablet, Phablet
Category 5	25W	Notebook
Category 6	37.5W	Regular laptop
Category 7	50W	

Table 2 PTU classifications

PTU Classes	Maximum Power Transfer	Minimum Category Support Requirements	Maximum Devices Supported
Class 1	2W	1 x Category 1	1 x Category 1
Class 2	10W	1 x Category 3	2 x Category 2
Class 3	16W	1 x Category 4	2 x Category 3
Class 4	33W	1 x Category 5	3 x Category 3
Class 5	50W	1 x Category 6	5 x Category 3
Class 6	70W	1 x Category 7	5 x Category 3

2.2 Resonant coupling

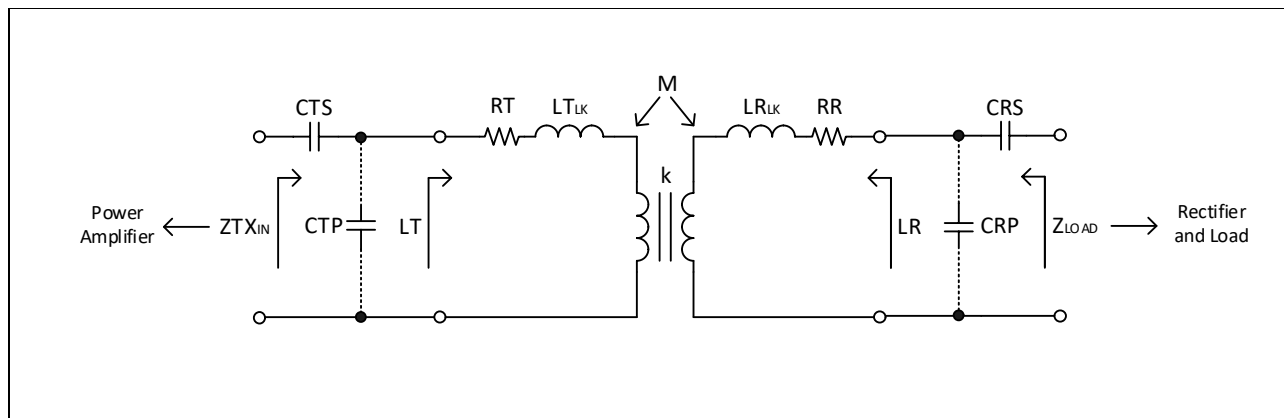


Figure 4 Transmit and receive coil coupling

The impedance tuning networks on both sides consist of series capacitors. Parallel capacitors are also sometimes added. The series capacitor values CTS and CRS are calculated based on the values of LT and LR and the resonant frequency of 6.78MHz. Shunt capacitors CTP and CRP may be added to increase the impedance. RT and RR represent the series DC resistance in each of the coils.

$$CTS = \frac{1}{4\pi^2 f^2 LT} \text{ and } CRS = \frac{1}{4\pi^2 f^2 LR} \quad [F] \quad [4]$$

The effect of the series impedance matching capacitor CTS is shown below:

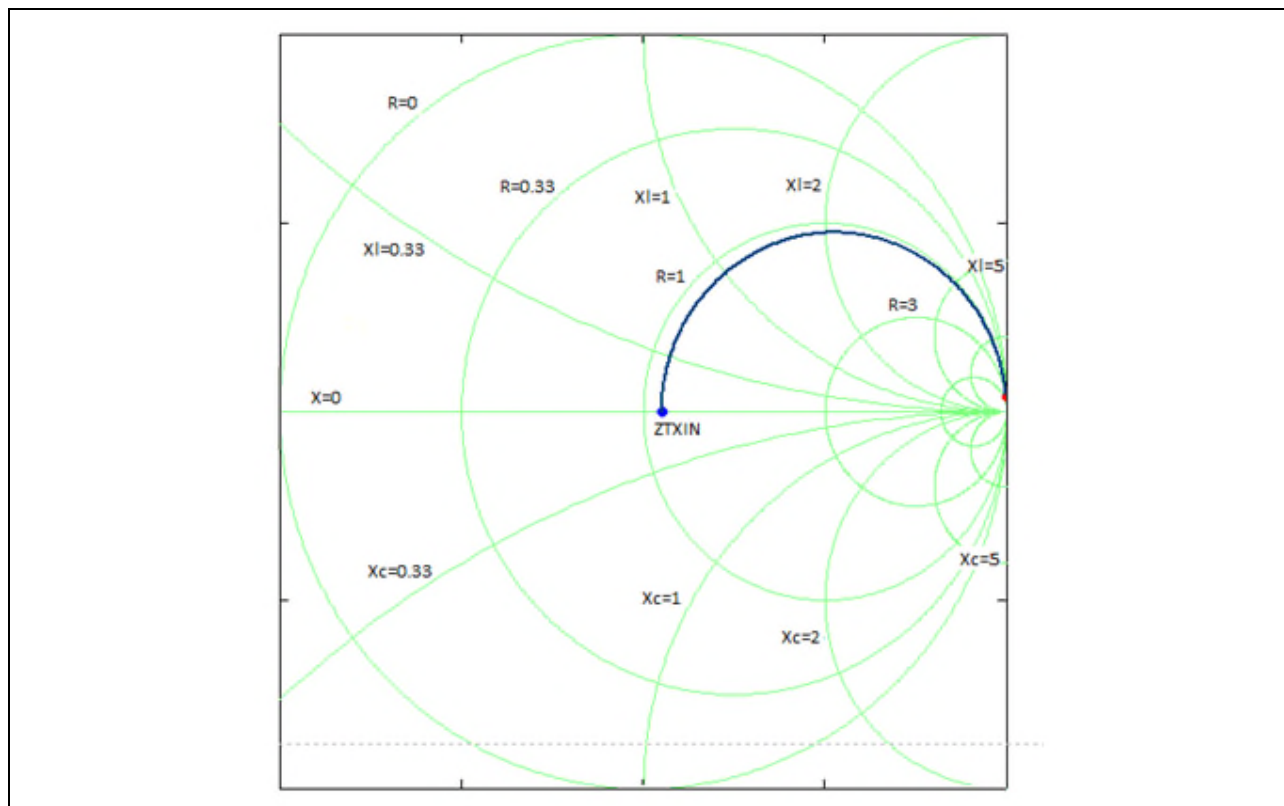


Figure 5 Z_{TXIN} Impedance Smith Chart

Air Fuel resonant wireless charging overview

The impedance Smith chart is plotted at 6.78MHz to illustrate the effect of adding CTP. The circles represent constant values of the resistive component of impedance and the curves originating from the right side represent reactive components above the center line for inductive and below for capacitive.

The red dot represents the lumped impedance looking into the transmit coil, which includes all of the elements shown to the right of the 'LT' arrow in figure 3. A set of typical values has been used to calculate this impedance value based on an example PTU and PRU which will be discussed later. Since the impedance contains a large inductive component due to the coil inductances the dot appears close to the center right of the Smith chart. With the addition of CTP the inductive component is cancelled and the impedance transformed to a purely resistive value represented by the blue dot. It can be seen that the resistive component is slightly more than 1Ω .

The output section consists of a bridge rectifier with a smoothing capacitor connected to a DC load. In a real application the DC load will vary, therefore the overall load is represented as an impedance Z_{LOAD} that may fall within a range of values bounded by four corners.

The effects of varying load, coupling factor 'k' and other component values can be demonstrated through an AC sweep of the network using the simulation setup shown below to produce a Bode plot. This can also be set up to produce a bode plot of the impedance Z_{TX_IN} , which is done by measuring the input current in relation to the input voltage.

The coupling factor 'k' is typically lies between 0.02 and 0.2. Higher values of 'k' create increased damping and splitting into two resonant peaks. The simulation shown below for varying values of 'k' illustrates this effect. It is important for the wireless charging system to remain tuned to resonance to obtain optimum power transfer efficiency. The circuit requires tuning adjustment for short distance (high 'k') operation.

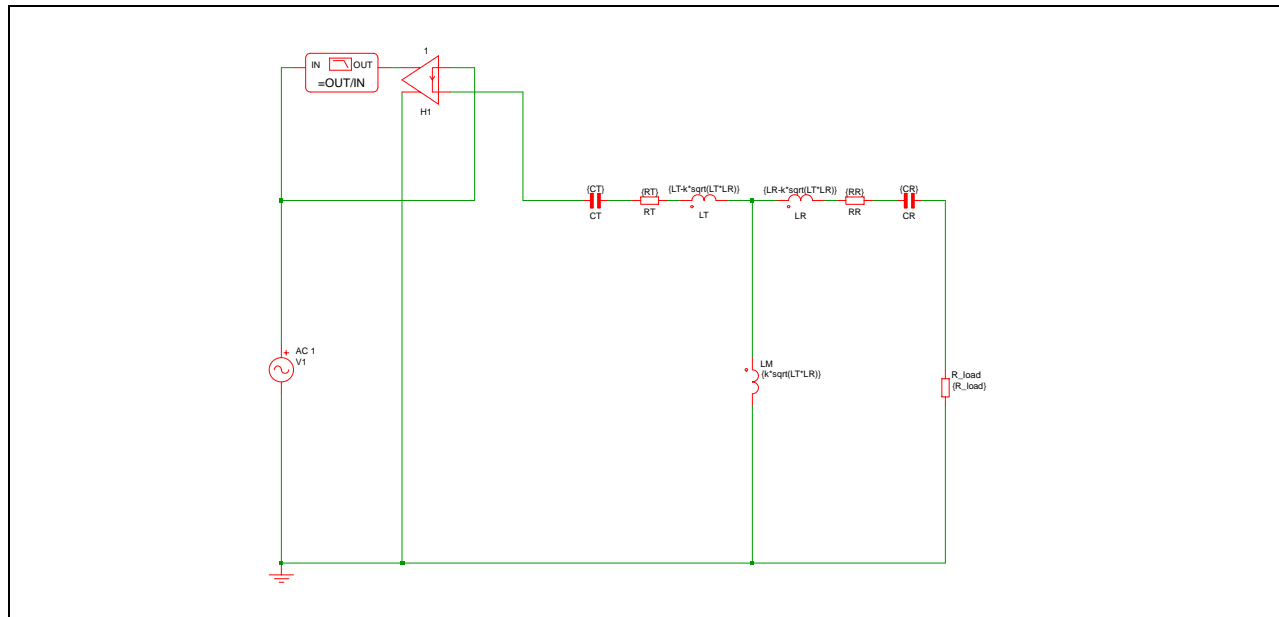


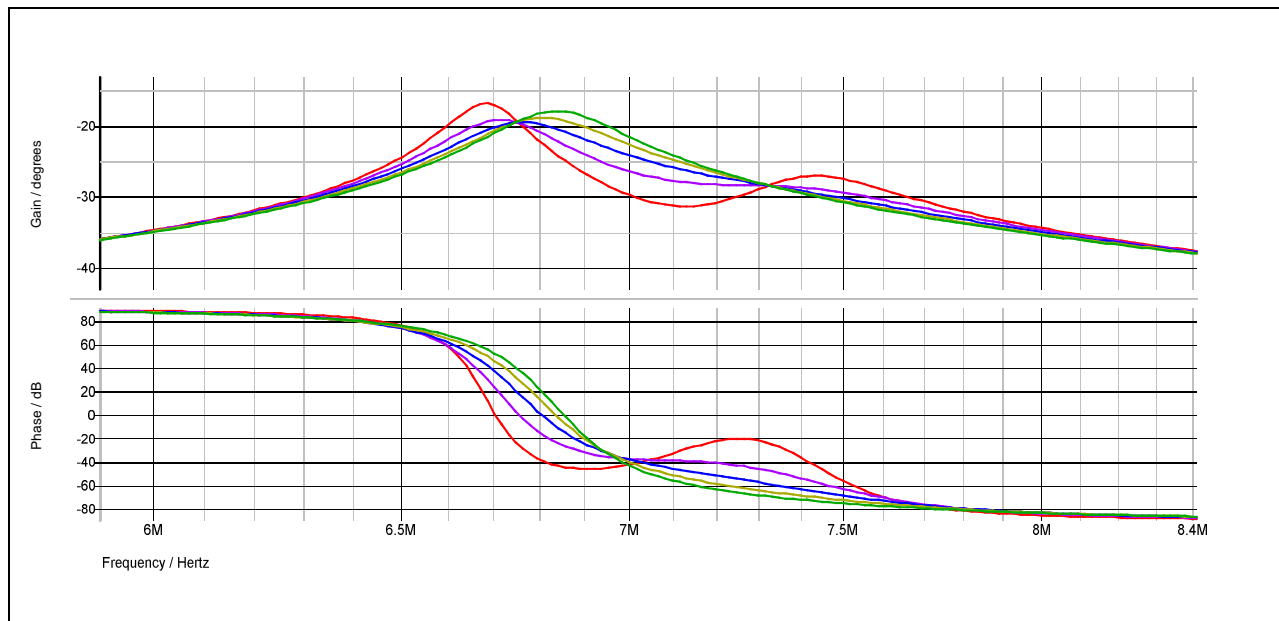
Figure 6 Transmit and receive coil coupling

The following impedance Bode plot shows the effect of different resistive loads connected to the output. The phase passes through zero at resonance, at which point Z_{TX_IN} appears purely resistive. It is also seen that variation of the load resistance causes a small shift in the resonant frequency.

In the following simulation examples, the following circuit values are used:

$$Z_{LOAD}=R_{LOAD}=25\Omega, CT=109\text{pF}, RT=1\Omega, LT=4.9\mu\text{H}, CR=220\text{pF}, RR=2\Omega, LR=2.25\mu\text{H}$$

Air Fuel resonant wireless charging overview

**Figure 7** Input impedance (Z_{tx_in}) vs Rload**Table 3** Load resistance trace colors

Rload	Trace Color
5	Red
10	Purple
15	Blue
20	Yellow
25	Green

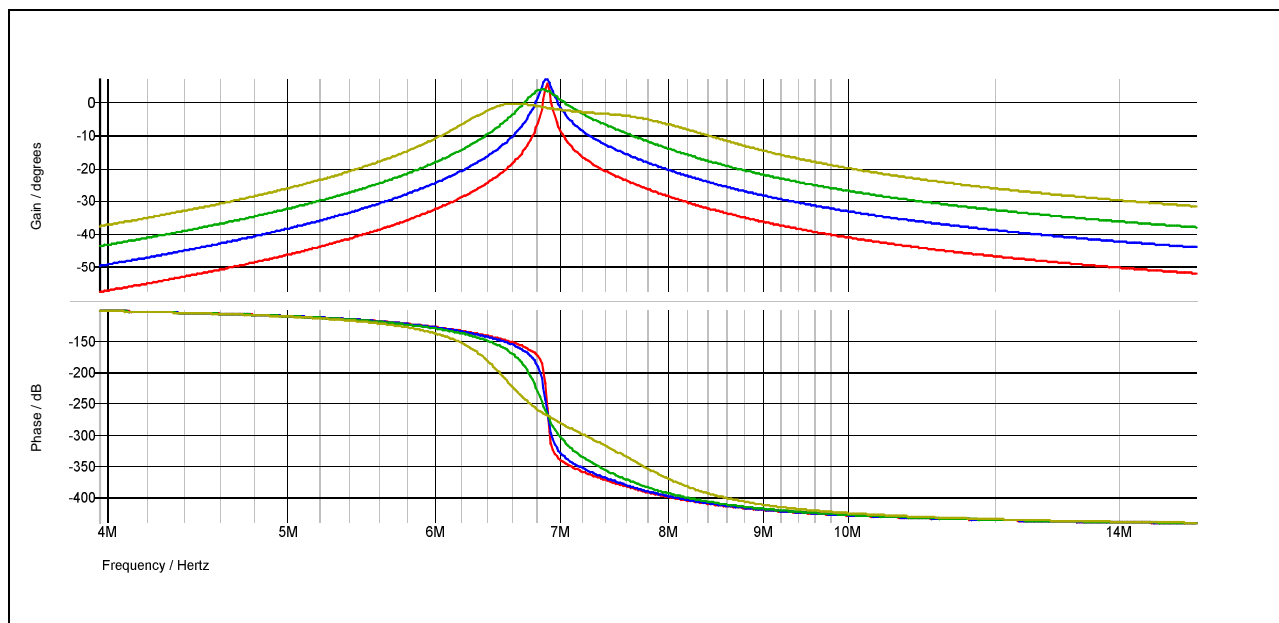
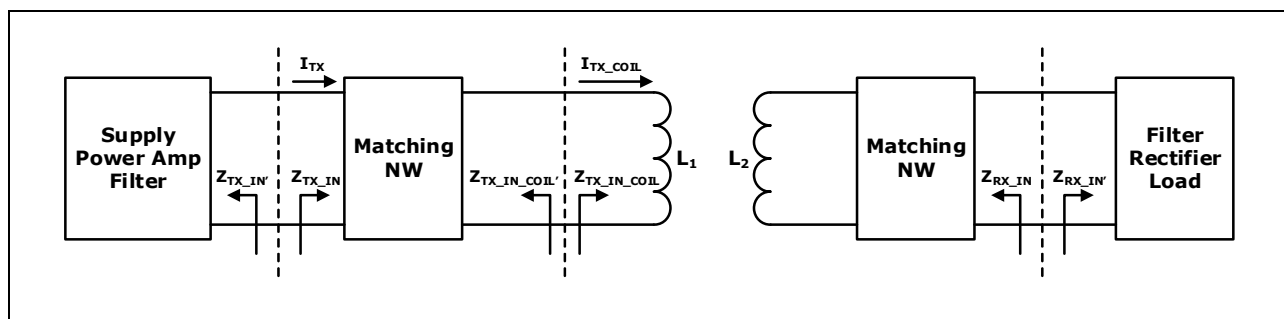
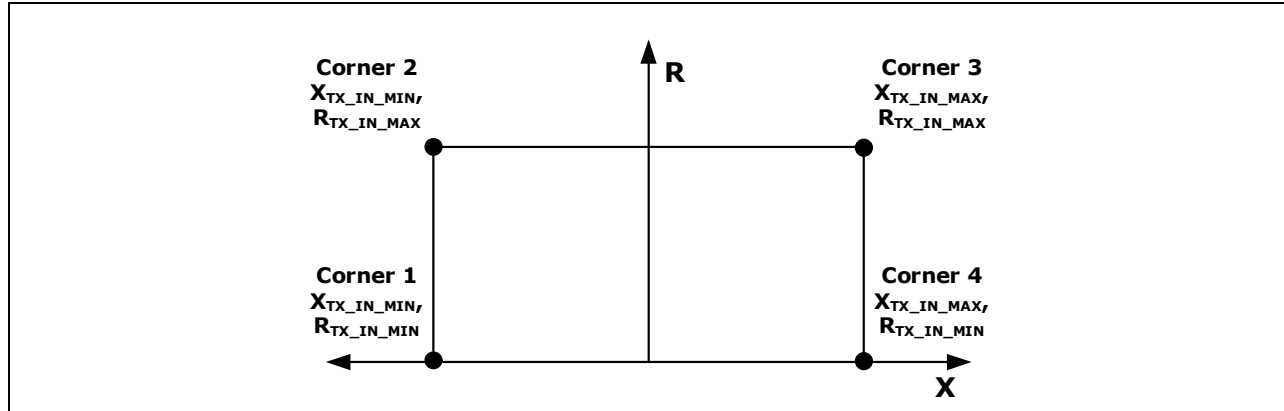
**Figure 8** Results of varying coupling factor 'k'

Table 4 Coupling factor trace colors

Coupling Factor 'k'	Trace Color
0.02	Red
0.05	Blue
0.1	Green
0.2	Yellow

Tuning is altered as the value of 'k' increases therefore the distance between the PTU and PRU coils for resonant inductive coupling systems affects circuit resonance, since 'k' varies inversely with distance.

**Figure 9 System impedances [1]****Figure 10 PTU resonator load impedance (Z_{TX_IN}) box [1]**

$$R_{TX_IN_MIN} \leq R_e\{Z_{TX_IN}\} \leq R_{TX_IN_MAX} \quad [\Omega] \quad [5]$$

$$X_{TX_IN_MIN} \leq I_m\{Z_{TX_IN}\} \leq X_{TX_IN_MAX} \quad [\Omega] \quad [6]$$

Air Fuel resonant wireless charging overview

The impedance driven by the power amplifier Z_{TX_IN} can be derived from the circuit elements shown in figure 3 (excluding the shunt capacitors CTP and CRP). LT=L1 and LR=L2 from figure 7. This gives the following formula¹:

$$Z_{TX_IN}(\omega) = R_T + j \left(\omega L_T - \frac{1}{\omega C_{TS}} \right) + \left(k \cdot \frac{\omega}{\omega_{RES}} \right)^2 \cdot \frac{\omega^2 \cdot L_T \cdot C_{RS} (R_R + R_{LOAD}) + j \omega L_T (1 - (\frac{\omega}{\omega_{RES}})^2)}{(1 - (\frac{\omega}{\omega_{RES}})^2)^2 + \omega^2 (C_{RS} (R_R + R_{LOAD}))^2} \quad [\Omega] \quad [7]$$

At resonance ω is equal to ω_{RES} allowing the equation to be simplified to:

$$Z_{TX_IN}(\omega_{RES}) = R_T + \frac{k^2 L_T}{C_{RS} (R_R + R_{LOAD})} \quad [\Omega] \quad [8]$$

Which can also be written in the form:

$$Z_{TX_IN}(\omega_{RES}) = R_T + \frac{\omega^2 M^2}{R_R + R_{LOAD}} \quad [\Omega] \quad [9]$$

As seen Z_{TX_IN} will be purely resistive only at resonance. The formula indicates that the reflected impedance seen by the power amplifier is inversely proportional to the actual load resistance. RT and RR are small in comparison. It should be noted that the point of resonance shifts with varying values of k and R_{LOAD} shown in figures 7 and 8. As R_{LOAD} reduces and the point of resonance shifts equations [8] and [9] no longer apply unless the circuit values are adjusted. For a fixed set of values Z_{TX_IN} increases as R_{LOAD} is reduced until a certain point is reached below which Z_{TX_IN} starts to drop with R_{LOAD}.

Larger reflected impedance is preferable for transferring power at higher efficiency because this requires lower voltage to be induced at the receiving coil. Resonator coupling efficiency (RCE) is defined as the maximum of the power delivered by the PRU to the load divided by the power delivered to the PTU coil at 6.78MHz.

To comply with the BSS the following minimum RCE values must be met:

Table 5 Minimum RCE (%) and dB between PRU and PTU [1]

	Category 1	Category 2	Category 3	Category 4	Category 5	Category 6	Category 7
Class 1	N/A						
Class 2	N/A	74% (-1.3)	74% (-1.3)	N/A	N/A	N/A	N/A
Class 3	N/A	74% (-1.3)	74% (-1.3)	76% (-1.2)	N/A	N/A	N/A
Class 4	N/A	50% (-3.0)	65% (-1.9)	73% (-1.4)	76% (-1.2)	N/A	N/A
Class 5	N/A	40% (-4.0)	60% (-2.2)	63% (-2.0)	73% (-1.4)	76% (-1.2)	N/A
Class 6	N/A	30% (-5.2)	50% (-3.0)	54% (-2.7)	63% (-2.0)	73% (-1.4)	76% (-1.2)

¹ Equations [7] to [9] derived by Matthias Brandl (MCI Management Center Innsbruck and Infineon Technologies AG)

2.3 PTU specifications

Suppliers of PTU resonators provide impedance boxes as shown in figure 8 by characterizing according to a series of standardized resonator acceptance tests (RATs). These tests are carried out using resonator interface testers (RITs), which are reference loads defined according to the BSS [1]. RITs are constructed from Aluminum or Copper blocks with some Ferrite shielding to simulate the load characteristics of PDs such as cell phones and tablets. PTU resonators are tested with different RITs to represent a range of load conditions. Impedance measurements are then plotted on a single impedance graph as depicted in figure 8, which is composed of a vertical real axis (R) for the resistive component and a horizontal imaginary axis for the reactive component (X). The impedance box is then added to enclose all of the impedance values with a small margin.

Apart from the impedance box the resonator coils inductance is specified to give LT as well as the Q factor, which may be used to calculate the resistance RT (referring to figures 2 and 3):

$$Q_{LT} = \frac{2\pi f LT}{RT} \quad [10]$$

$$RT = \frac{2\pi f LT}{Q_{LT}} \quad [\Omega] \quad [11]$$

LT is used to calculate the value of the series impedance matching capacitor (CTS) using equation [4].

3 Class-E power amplifier

The class-E amplifier offers better efficiency at the design operating point than other topologies such as the class-D amplifier, while requiring only one power switch in the single ended (SE) implementation rather than the two used in class-D. A two switch differential (DE) class-E topology is used at higher power levels to produce twice as much output voltage and therefore four times as much power into a given load.

Optimum class-E operation requires the following three conditions to be met [4]:

- The rise of the voltage across the transistor (Q1) at turn-off should be delayed until after the transistor is off.
- The drain (or collector) voltage should be brought back to zero at the time of transistor turn-on.
- The slope of the drain voltage should ideally be zero at the time of turn-on.

The single ended class-E RF power amplifier topology is as follows:

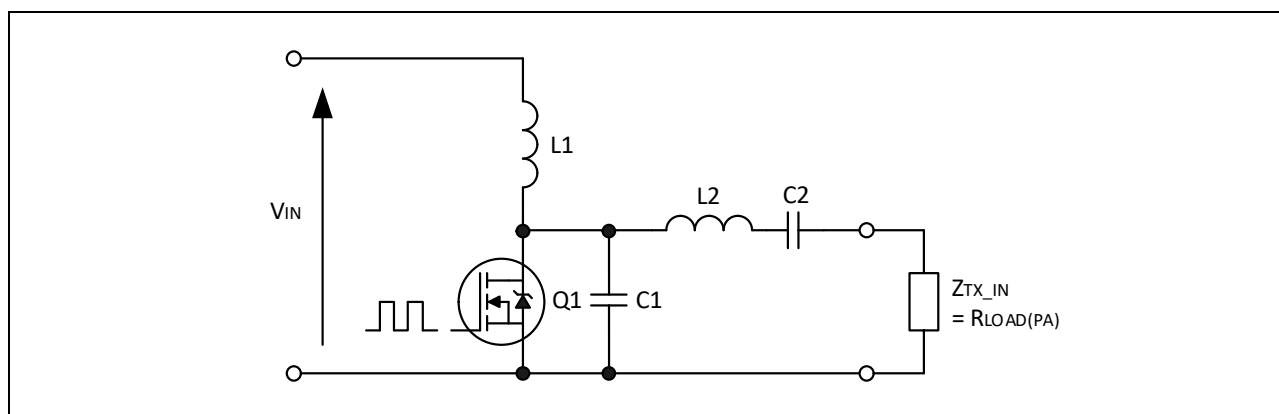


Figure 11 Single ended class-E amplifier

In the Air Fuel wireless charging application the gate of power switch Q1 is driven with a 6.78MHz square wave. The circuit design goal is to operate with zero voltage switching (ZVS) over the range of load impedance values defined (see figure 10). The power amplifier output sees the impedance Z_{TX_IN} . Since this is tuned to resonance as previously described, it appears as a purely resistive value $R_{LOAD(PA)}$ not to be confused with Z_{LOAD} or R_{LOAD} (as defined in this paper) as seen by the receiver circuit.

To accomplish ZVS Q1 needs to be selected for low output capacitance C_{OSS} (defined as $C_{DS} + C_{GD}$). $C1$ should have a tolerance of +/-10% or less, with capacitance larger than C_{OSS} to reduce the effect of the non-linearity of C_{OSS} with respect to drain to source voltage as well as its tolerance. However the combined capacitance from the drain to the source ($C_{OSS} + C1$) needs to remain below a certain limit for ZVS to be possible for higher $R_{LOAD(PA)}$ values and to meet the design criteria, which will be explained further on.

Partial hard switching typically occurs under lighter load conditions. Switch on losses can be calculated as follows:

$$P_{SW} = \frac{1}{2} \cdot C_{OSS} \cdot V_{DS}^2 \cdot f_{SW} \quad [W] \quad [12]$$

Class-E power amplifier

Where V_{DS} refers to the drain voltage immediately before switch on (zero under a true ZVS condition) and C_{oss} is the value at that V_{DS} level, which can be extrapolated from the MOSFET datasheet graph of C_{oss} against V_{DS} (note that the listed value is usually at half $V_{(BR)DSS}$).

The output power is given by:

$$P_{OUT} = I_{OUT}^2 \cdot R_{LOAD(PA)} = \frac{V_{OUT}^2}{R_{LOAD(PA)}} \quad [W] \quad [13]$$

The class-E PA operating in ZVS behaves like an AC current source where I_{OUT} does not change much as the value of $R_{LOAD(PA)}$ varies. It should be noted that ZVS operation is not possible above a certain $R_{LOAD(PA)}$ maximum value and that when driving an open-circuit load the drain voltage waveform will assume an exponential shape and hard switching will occur. It is important to avoid this condition or include protection circuitry to prevent overheating and failure of Q1 under this condition such as hiccup mode protection.

Two key properties of the class-E PA operating in ZVS are:

1. I_{OUT} varies proportionally with the DC input voltage V_{IN} (for fixed values of $R_{LOAD(PA)}$, L1, C1, L2 and C2)
2. I_{IN} varies proportionally with V_{IN} for a specific load. Therefore I_{OUT} also varies proportionally with I_{IN} .

Therefore since P_{OUT} is proportional to $R_{LOAD(PA)}$, V_{IN} must be increased proportionally as $R_{LOAD(PA)}$ is reduced to maintain a constant output power. The minimum value for $R_{LOAD(PA)}$ driven at a given power is then determined by the maximum drain-source voltage rating of Q1.

3.1 Passive component selection

The DC input voltage bus to drain inductor (L1) must a high enough value to provide a roughly constant current to the circuit, the average of which will be equal to the DC bus input current. This current is conducted to ground when Q1 is on and shared between C_{oss} , C1 and L1 when Q1 is off. The value of L1 does not have to be precise and is selected by a tradeoff between highest inductance and current carrying capability for the required power transfer class. A ferrite drum core inductor is normally sufficient.

The minimum acceptable value for L1 may be determined as follows:

$$L1_{MIN} = \frac{(\pi^2+4) \cdot R_{LOAD(PA)}}{f_{sw}} \quad [\mu H] \quad [13]$$

Two distinct resonant frequencies exist in the class-E circuit; f_{r1} , which occurs when the Q1 is closed where Q1 shorts out C1 and C_{oss} , and f_{r2} , which occurs when the Q1 is open therefore including C1 and C_{oss} :

$$f_{r1} = \frac{1}{2\pi\sqrt{L2 \cdot C2}} \quad [\text{MHz}] \quad [14]$$

$$f_{r2} = \frac{1}{2\pi\sqrt{L2 \cdot C_{eq}}} \quad [\text{MHz}] \quad [15]$$

Where

$$C_{eq} = \frac{(C1 + C_{oss}) \cdot C2}{C1 + C_{oss} + C2} \quad [\text{pF}] \quad [16]$$

Class-E power amplifier

The impedances of L2 and C2 should not be too high to avoid overheating. To avoid this, the value of L2 should be kept low and the value of C2 should be kept high.

One necessary condition for ZVS switch on is that fr1 be lower than the switching frequency, which needs to be lower than fr2:

$$fr1 < f_{sw} < fr2 \quad [\text{MHz}] \quad [17]$$

Another condition is that the sum of half of one period of fr1 and fr2 should be close to the period of fsw:

$$\frac{1}{2 \cdot fr1} + \frac{1}{2 \cdot fr2} \approx \frac{1}{f_{sw}} \quad [\text{ns}] \quad [18]$$

For correct results in practice the sum of the terms on the left of equation [18] is slightly higher than the reciprocal of fsw.

The drain current waveform shape depends on the loaded quality factor QL such that it will follow an approximately sinusoidal shape only if QL is greater than approximately 2.5, otherwise it will look exponential resulting in hard switching.

The PA output inductor (L2) value along with C2 and C1 must be carefully selected to achieve the desired ZVS operation in the desired operating range. C2 will have a high peak to peak voltage across it and needs to support the output current so it must be rated to >500V with low loss and high stability. Equations [14] through [17] may be used to arrive at an initial set of component values, however due to the tolerance and non-linearity of C_{oss} some fine tuning of the circuit will probably be necessary. The suggested design approach is first to simulate and then to make the final adjustments with the actual circuit in the laboratory.

It is essential that capacitors suited for resonant applications with high Q, low ESR at frequencies in the MHz range and good temperature stability are used in the circuit. High voltage COG dielectric capacitors are recommended.

The values can be adjusted according to the shape of the drain voltage waveform according to the method devised by N. Sokal [3] as illustrated in the following diagrams. This provides an extremely helpful guide to which components should be adjusted to tailor the waveform to the desired ZVS shape.

Class-E power amplifier

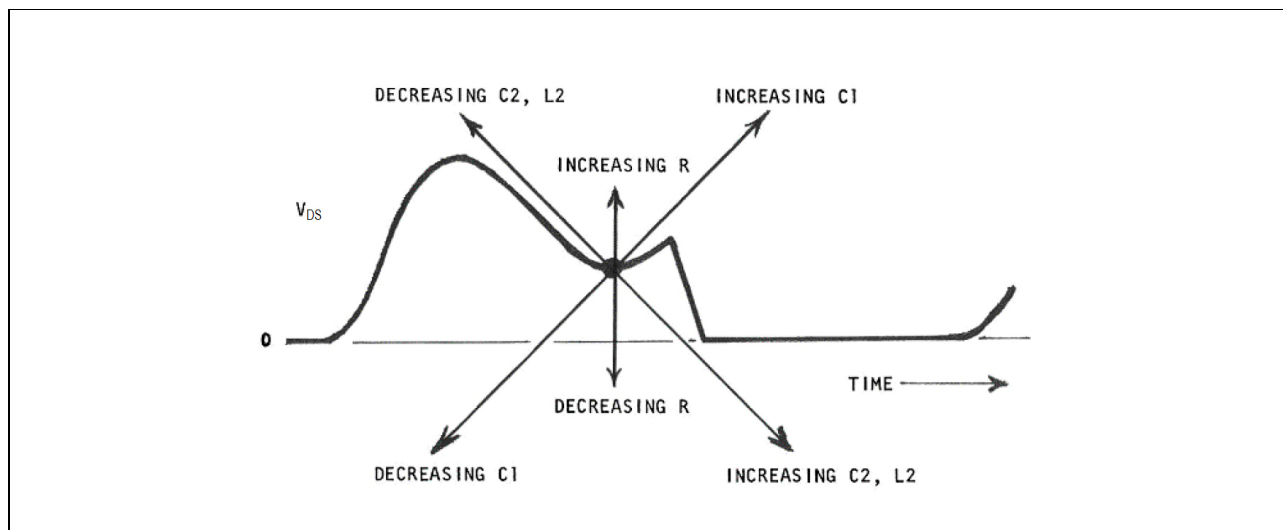


Figure 12 Effects of adjusting class-E PA component values

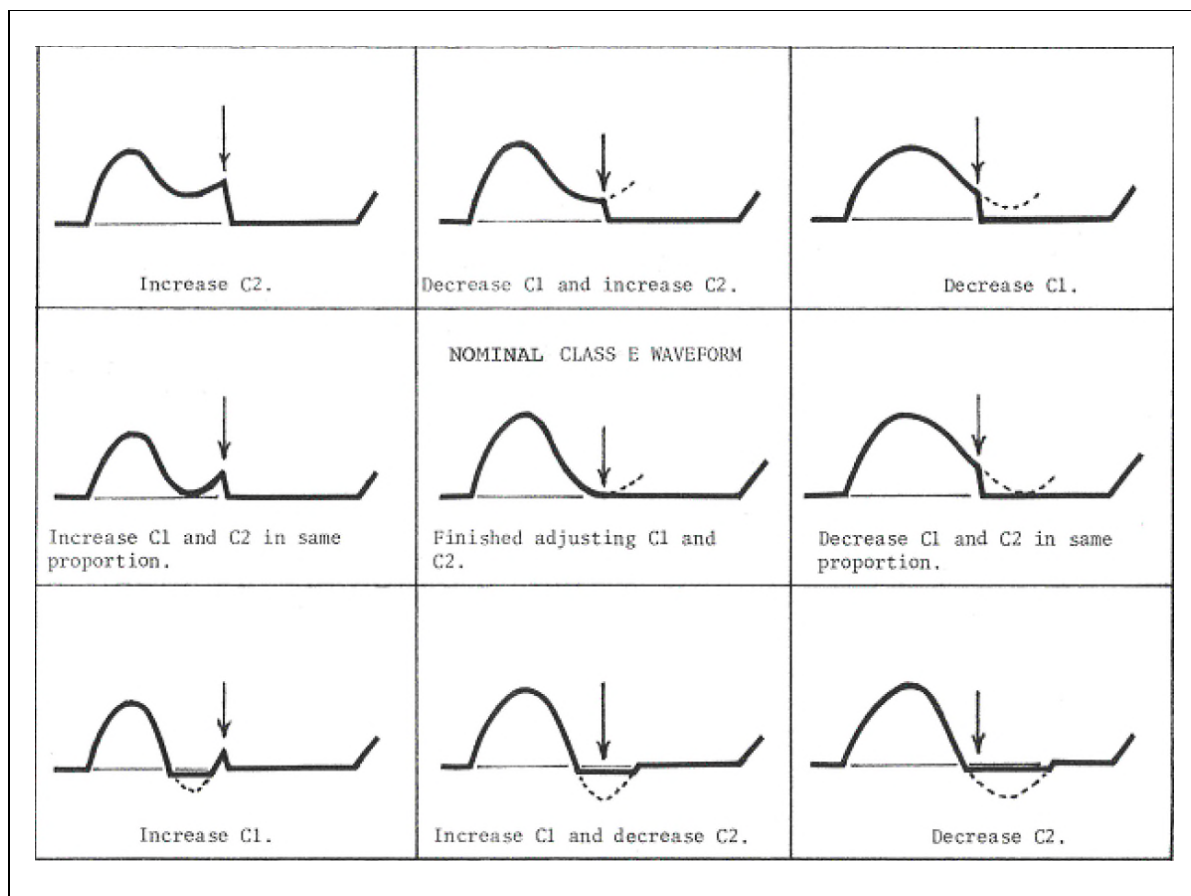


Figure 13 C1 and C2 adjustment procedure (The arrow indicates the point of Q1 switch on)

3.2 MOSFET selection

The maximum V_{IN} needed as a function of output power and load impedance previously discussed. The highest V_{IN} is required for maximum output power and highest ZTX_{IN} considering that ZTX_{IN} increases as the load resistance R_{LOAD} is reduced according to equation [9]. Please remember that R_{LOAD} refers to the output for the complete system including both transmit and receive coils with their respective impedance matching networks, which is distinct from $R_{LOAD(PA)}$ that refers a resistive load connected directly to the PA output.

To determine the required MOSFET $V_{(BR)DSS}$ the minimum value of ZTX_{IN} should be considered since this results in the highest drain voltage peak. This can be calculated from equations [8] and [9] using simulation to verify then some safety margin should be added. It is important to keep in mind that in the class-E PA that allowing the peak drain voltage to exceed the breakdown voltage rating of a Silicon MOSFET device results in avalanching and high risk of destruction!¹

Under normal operation, the power switch (Q1) needs to be rated high enough to withstand a drain to source voltage (V_{DS}) of at least 3.56 times the maximum value of V_{IN} . However if the system is incorrectly tuned or a load is applied outside of the design range, voltages up to 7 times V_{IN} could be present. These conditions must be avoided unless a MOSFET with much higher voltage rating is used, which is undesirable because of higher C_{oss} and/or $R_{DS(on)}$.

The required MOSFET voltage rating can be calculated based on the maximum value of V_{IN} :

$$V_{(BR)DSS} > 3.56 \cdot V_{IN} + V_{SM} \quad [V] \quad [19]$$

Where, V_{SM} is a safety margin which is recommended at $\geq 20\%$. This is based on the assumption that the system is designed to avoid undesired load conditions where the drain voltage would peak to higher voltages.

The next critical MOSFET parameter is the output capacitance C_{oss} . For a specific operating condition, the maximum value of $C_1 + C_{oss}$ can be determined from the formula provided by N. Sokal:

$$C_1 + C_{oss} = \frac{8}{(2\pi f)\pi(\pi^2+4)ZTX_{IN}} = \frac{0.1836}{2\pi f \cdot ZTX_{IN}} \quad [pF] \quad [20]$$

This should be calculated for the maximum value of ZTX_{IN} used to determine the maximum value of V_{IN} above. Ideally a value of C_{oss} significantly lower than the result of the above equation should be chosen so that $C_1 \gg C_{oss}$. It should be remembered that C_{oss} ² is voltage dependent, increasing significantly at lower V_{DS} . In a practical class-E circuit this causes slope of the negative transition of the drain voltage to change as the voltage approaches zero. This effect is clearly seen in the drain voltage waveform, often resulting in switch on of the MOSFET while a small V_{DS} is present. Although this does not meet the requirement (b) for optimum class-E operation, it does not usually result in excessive power losses provided the level of hard-switched voltage remains small (not more than 20V).

¹ Gallium Nitride (GaN) FETs do not exhibit avalanche breakdown, however exceeding the maximum rated drain-source voltage risks reducing operating lifetime.

² C_{oss} is typically specified at a V_{DS} of 50% of the maximum rated drain-source voltage in MOSFET data sheets.

Class-E power amplifier

The voltage and current appearing at ZTX_{IN} are sinusoidal if the resonator networks are correctly tuned. These values may be calculated as follows:

$$V_{TX(RMS)} = \sqrt{P_{TX}ZTX_{IN}} \quad [V] \quad [21]$$

$$I_{TX(RMS)} = \sqrt{\frac{P_{TX}}{ZTX_{IN}}} \quad [A] \quad [22]$$

For the purposes of estimating the current required for the MOSFET, the drain peak current can be taken to be approximately equal to the peak current entering ZTX_{IN} .

Low gate charge (Q_G) is also a requirement for operation at 6.78MHz. The gate drive current and power consumption can be calculated by:

$$I_G = Q_G \cdot f_{SW} \quad [A] \quad [23]$$

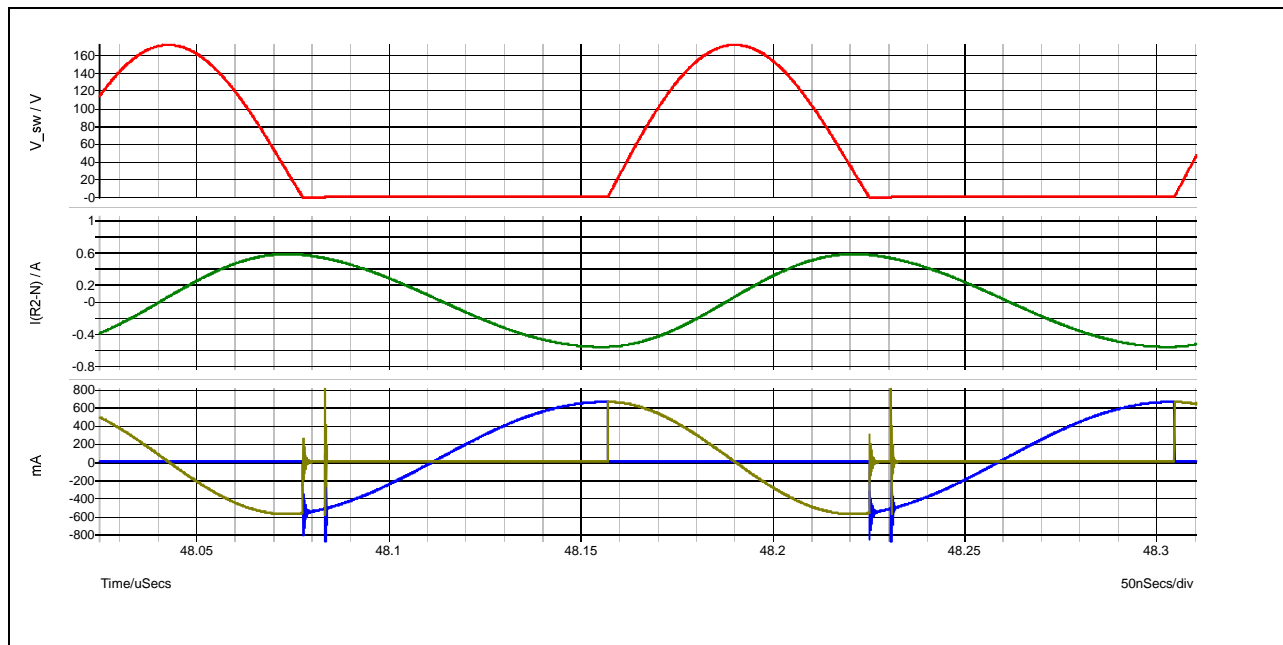
$$P_G = V_{DD} \cdot Q_G \cdot f_{SW} \quad [W] \quad [24]$$

Where, VDD is the supply voltage to the driver IC.

The waveforms shown below represent the currents and voltages in an ideal system operating from a 50V supply, where the MOSFET C_{oss} is a fixed value (the effects of the variation of C_{oss} with V_{DS} will be examined more closely). The drain voltage is shown in red indicates a peak voltage of 173V, which gives a ratio of 3.46 close to the value of 3.56 expected from the literature.

The green waveform represents the current passing through L2 into the ZTX_{IN} . The blue waveform shows the current flowing through the MOSFET (Q1) during its on period and the brown/yellow waveform shows the combined current shared between C_{oss} and C1. The combination of Q1 drain and parallel capacitor currents produces an approximately sinusoidal current 180° out of phase with the amplifier output current driving the impedance matching network and PTU represented by ZTX_{IN} .

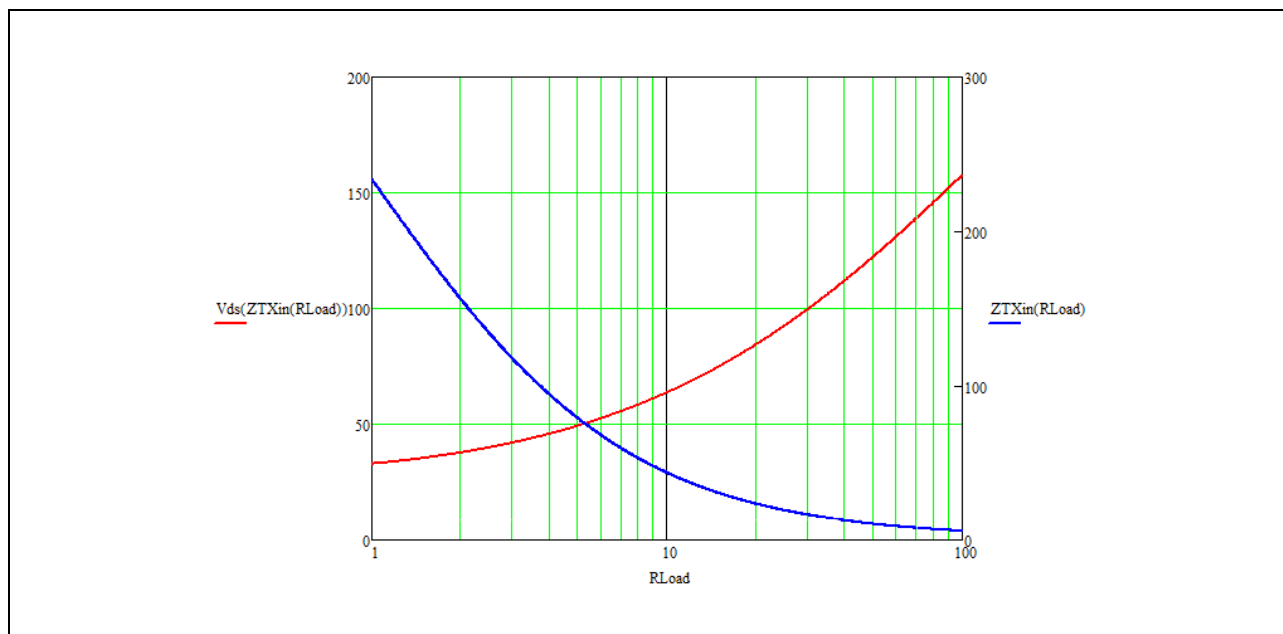
Class-E power amplifier

**Figure 12 Single ended class-E amplifier voltage and current waveforms**

The MOSFET $I_{D(\max)}$ rating required for the application can therefore be determined from equation [22] allowing sufficient headroom to handle non-ideal load conditions in which current also flows through the body diode for a portion of the conduction cycle.

An SMD MOSFET package is typically used, which should be chosen to adequately dissipate the heat generated by the conduction losses in conjunction with a large enough area of Copper on the PCB. The conduction loss can be estimated from the equations provided in conjunction with the $R_{DS(on)}$ of the device, where the RMS current can be taken as ~ 0.5 times the current calculated from equation [22].

Equations [13] and [14] are used to plot the peak drain voltage and Z_{TXIN} over a range of output loads for an example 16W class-E PA design:

**Figure 13 Peak drain voltage and Z_{TXIN} against load**

Class-E power amplifier

It can be seen that a 200V MOSFET is required to cover a range of loads down to 5Ω .

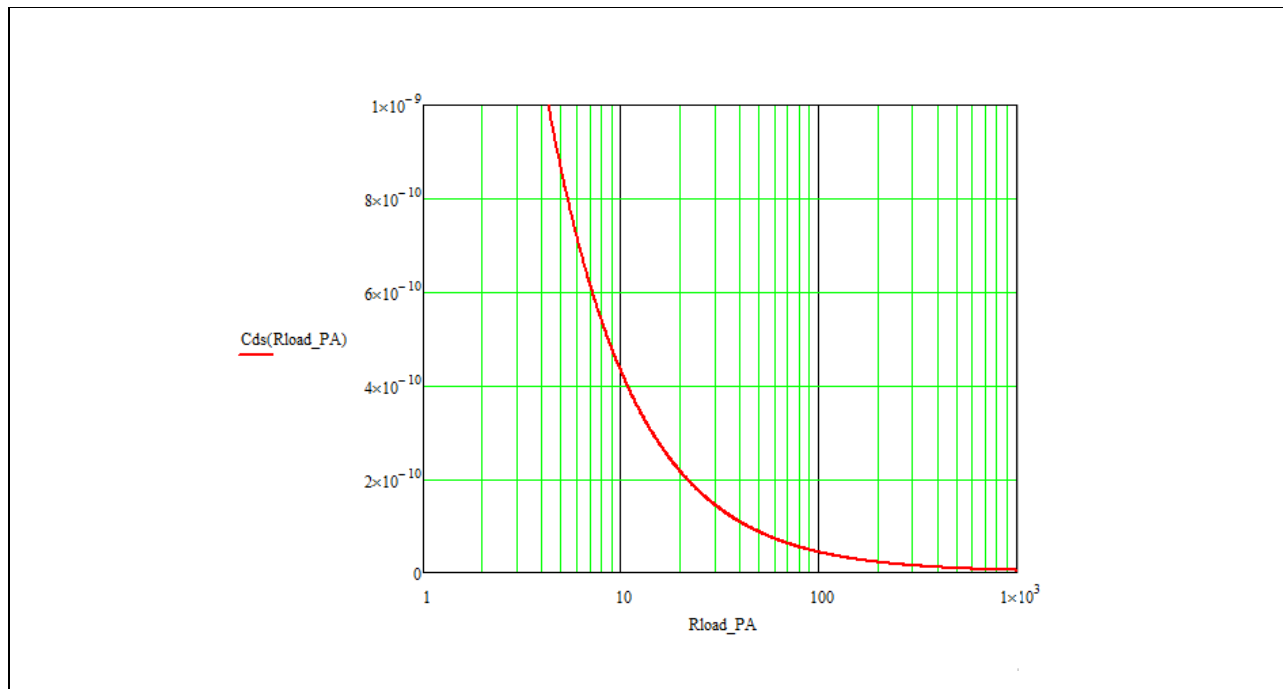


Figure 14 Drain-source capacitance values for different load conditions

It can also be seen that according to the formula the total drain-source capacitance ($C_{oss} + C1$) is limited to a value under 100pF at the 25Ω maximum load resistance.

3.3 Operation under varying load conditions

The class-E power amplifier is typically designed to operate at a fixed 50% duty cycle and optimized for a specific load condition. However in the application the load impedance varies depending on the number of PDs placed on the charging pad and their orientations resulting in an impedance box shown in figure 5.

As the load deviates from the design point the voltage and current waveforms become non-ideal.

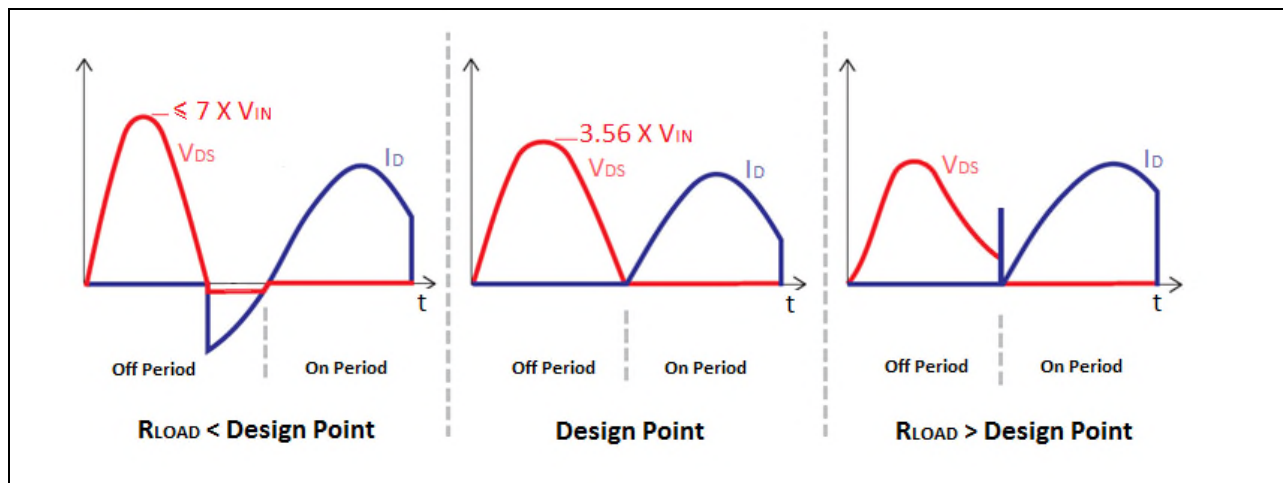


**Figure 15 Drain voltage and current under varying load conditions
(Diagram from Efficient Power Corporation – References [6])**

The above figure (left) illustrates that if the reflected load resistance is lower than the amplifier design point, the drain voltage peaks to a higher level and falls to zero before the end of the off period of Q1. At this point current begins to flow through the body diode until the gate drive switches on to begin the next cycle. This will also occur if the value of $C_{oss} + C_1$ is too low.

Under ideal conditions the drain voltage rises to 3.56 times the DC input voltage and then falls to reach zero at the point of switch on maintaining ZVS.

If the load resistance is higher than the design point the drain voltage does not fall all the way to zero before the end of the off period producing a hard switching condition with associated switch on current spike.

Depending on how far the load has deviated from the design point value, the level of hard switching may be quite low as shown above (right) or in extreme conditions it could be very high leading to severe switching losses and potential over-heating of the MOSFET. It should be possible to avoid this situation by designing the amplifier for a load close to the center of the required range of operation. It is advisable to also include some protection circuitry to detect extreme conditions and cause the amplifier to operate in hiccup mode until the load is restored to a state within design acceptable limits.

4 Simulated performance

4.1 Power amplifier driving a resistive load

The following simulation test circuit is used to evaluate the performance the BSC12DN200NS3 OptiMOS MOSFET in the class-E power amplifier using the Simetrix simulation tool. The component values are calculated according to the design equations from the previous section. The input voltage is adjusted to supply 16W to a resistive load of 25Ω and also 5Ω representing Z_{TXIN} . The value of C_1 is adjusted to obtain ZVS with lowest peak drain voltage for each load.

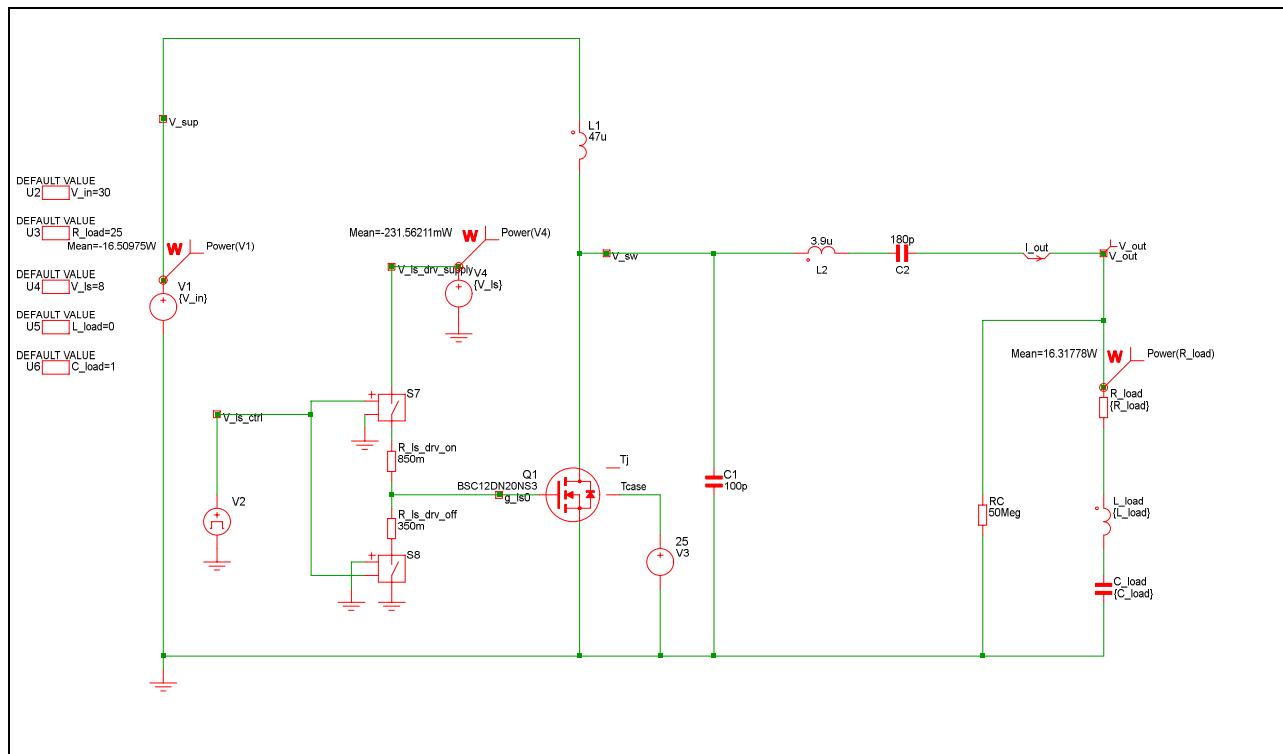
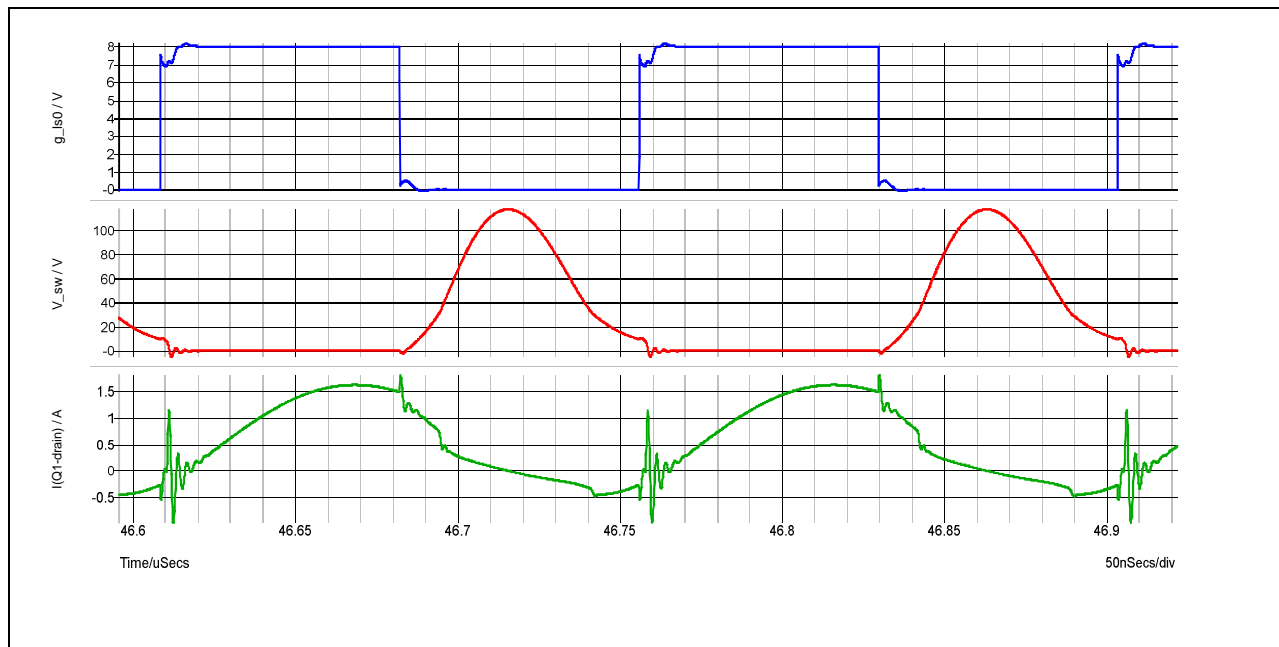
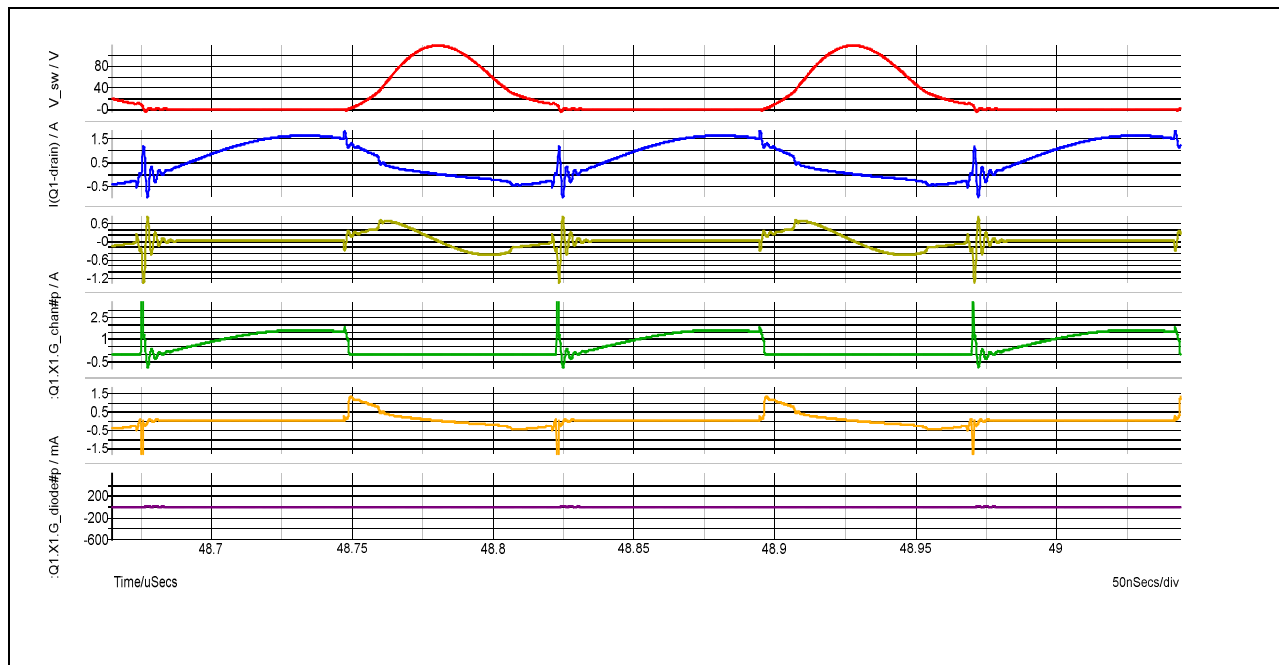


Figure 16 Simulation test platform

Simulated performance

Figure 17 Drain voltage and current waveforms for the BSC12DN200NS3 at 25Ω load

The blue trace above is the gate drive voltage, the red trace is the drain voltage and the green is the drain current. For a load of 25Ω the peak drain voltage is 117V for V_{IN} of 30V, which gives a ratio of 3.9 a little higher than the theoretical ratio of 3.56 given in the design formula. It can be seen that the system is operating close to ZVS but with a small amount $\sim 10V$ of hard switching, which causes a current spike at switch on. This occurs because the MOSFET C_{oss} increases as the drain to source voltage falls to lower levels as shown in the graph of C_{oss} against V_{DS} provided in MOSFET data sheets. It is possible to reduce hard switching by reducing C_1 , however this would result in a higher peak drain voltage, which would limit the operating load range therefore it is better to allow a trade-off between peak drain voltage and hard switching.

Figure 18 Drain current components for the BSC12DN200NS3 at 25Ω load

Simulated performance

The drain current measured is the total current entering the drain terminal of the MOSFET, which is composed of channel current when the MOSFET is switched on and a combination of body diode current and C_{oss} current when it is switched off.

The components of the drain current are shown in the above figure as follows:

Table 6 MOSFET and C1 voltage and current waveforms

Signal	Trace color
Drain voltage	Red
Total drain current	Blue
Channel current	Green
Body diode current	Purple
C_{oss} current	Orange
C1 current	Yellow

The simulation results show that the body diode does not conduct current when the PA is operating close to the ZVS state. It is seen that current flows through C_{oss} and C1 only during the off period and through the channel during the on period. During the off period the PA output current is composed of C_{oss} + C1 currents.

The simulation is also carried out with a 5Ω load with the input voltage VIN increased to provide 16W at the load.

In this case the peak drain voltage increases. It was found that C1 needed to be increased to prevent the drain voltage exceeding the MOSFET drain-source maximum rating VDSS(BR) for 200V devices.

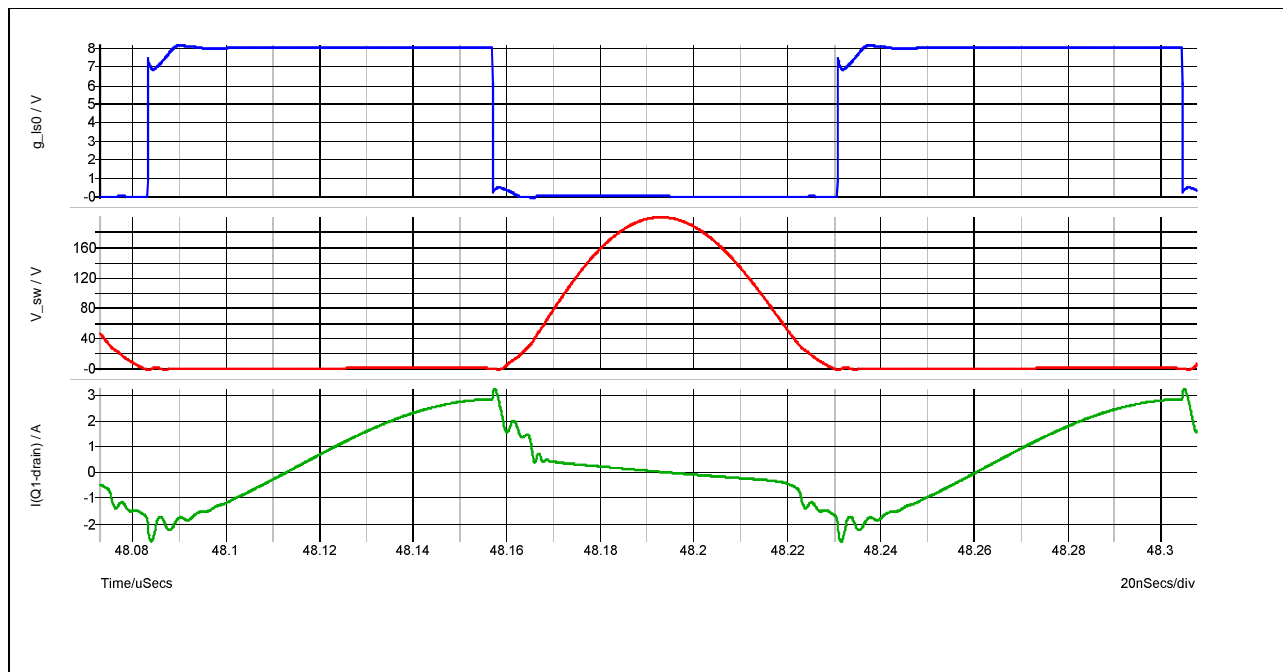


Figure 19 Drain voltage and current waveforms for the BSC12DN200NS3 at 5Ω load

Simulated performance

The ratio of peak drain voltage to input voltage is now 3.64, close to the theoretical ratio of 3.56 as a result of C1 having been increased from 100pF to 220pF. This indicates that the class-E PA has been adjusted to maintain operation close to the optimum, which limits the peak drain voltage to 200V for the BSC12DN20NS3 with a peak drain current increased to 3A. The higher current and value of C1 reduce the effect of C_{oss} variation such that hard switching does not occur.

The components of current are seen below:

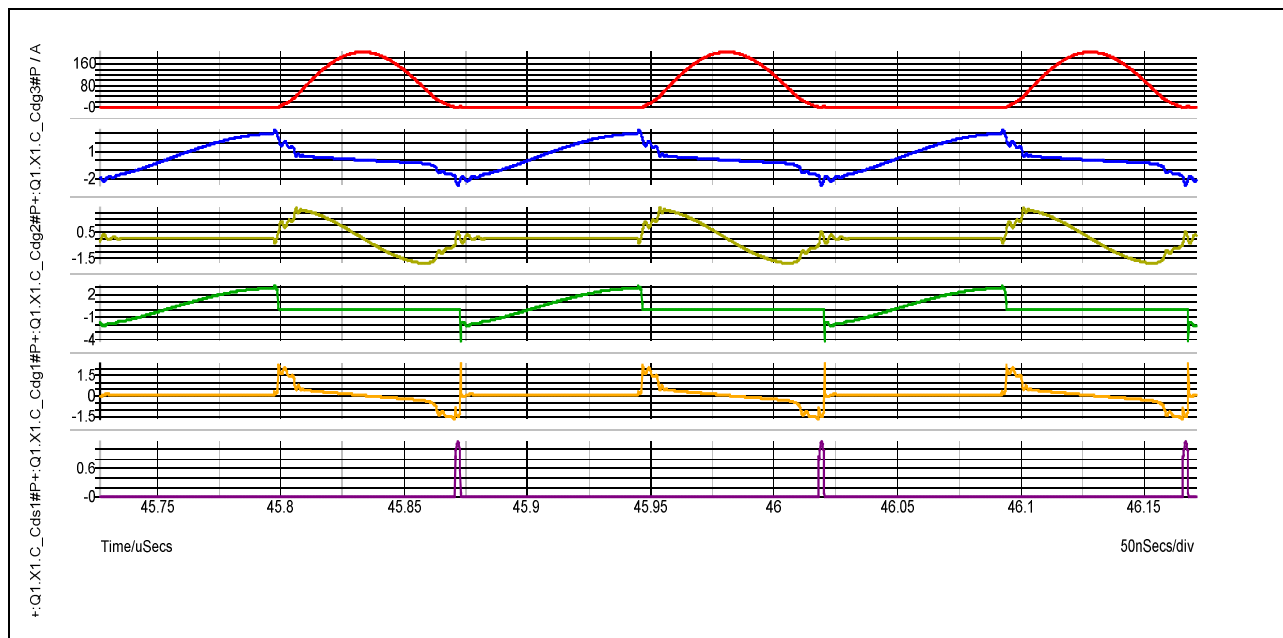


Figure 20 Drain current components for the BSC12DN200NS3 at 5Ω load

A transient body diode current spike is sometimes observed at switch on depending on the MOSFET type and value of C1. This occurs if the drain voltage briefly transitions below zero at switch on causing a short period of body diode conduction. This can be reduced by increasing value of the gate drive resistor if necessary.

Simulated performance**4.2 Complete system simulation**

The following single ended class-E PA simulation includes the transmit and receive coils with their respective impedance matching networks.

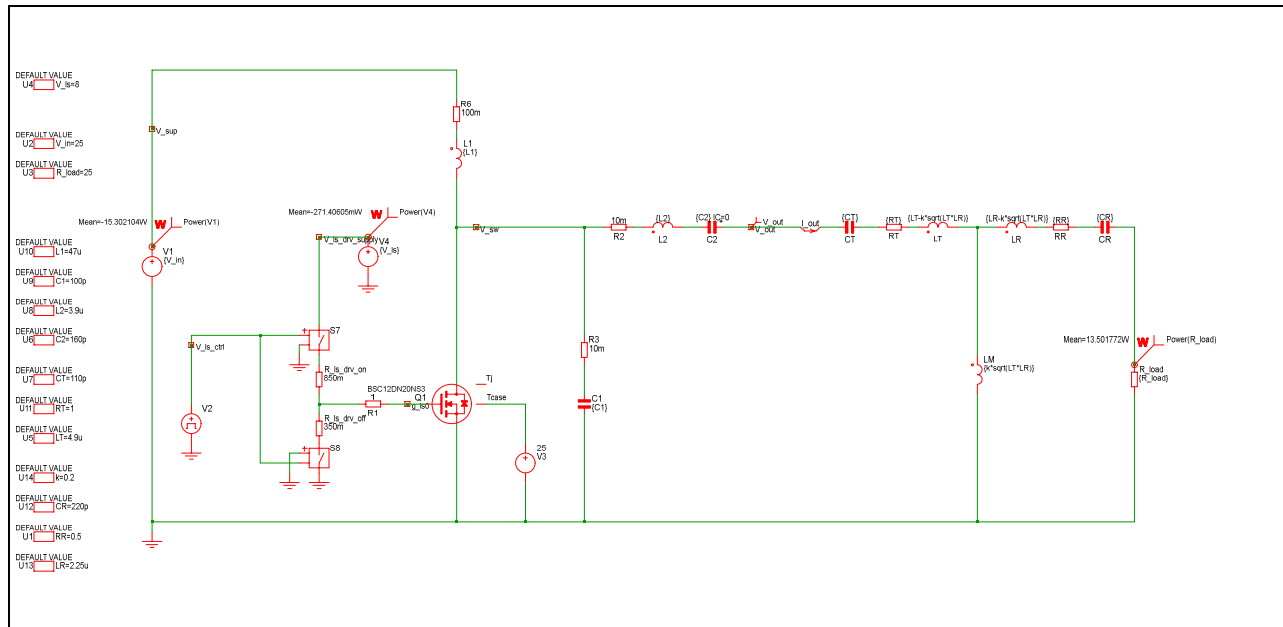


Figure 21 Simulation test platform

In this example the coupling factor 'k' has been set to 0.2 with 25Ω load resistance. The values of self and mutual inductances have been calculated according to equations [2] and [3]. CT and CR are selected for resonant operation. The values for the class-E circuit have been tuned to provide the best possible ZVS waveform at the drain of Q1.

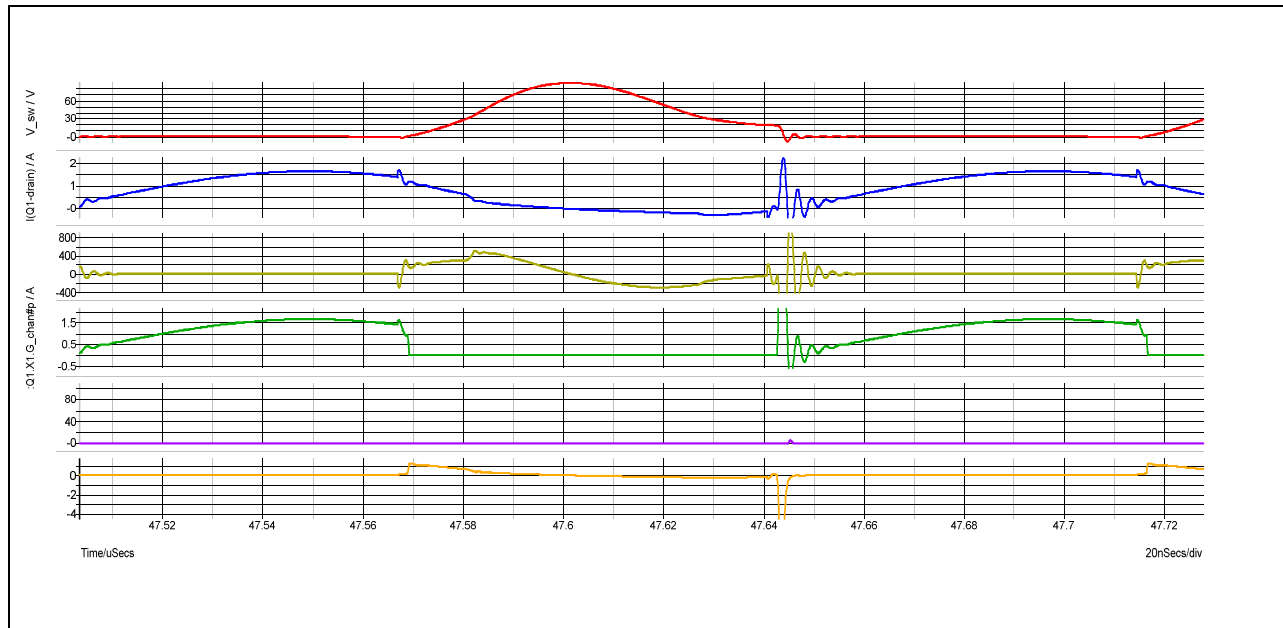


Figure 22 Circuit waveforms for $k=0.2$

Simulated performance

The waveforms follow the same color convention detailed in table 6. The peak drain voltage is 89.4V, which is 3.58 times the V_{IN} value of 25V and there is negligible body diode conduction indicating that the class-E PA is tuned very close to the optimum design point. As seen previously the increase of C_{oss} as the drain-source voltage falls slows down its negative going slope resulting in partial hard-switching of around 20V at switch on. According to the power probes the overall system efficiency is around 87%.

It is also seen from the following waveforms the output current from the PA entering the matching networks $I_{OUT(PA)}$ (green) is sinusoidal though the voltage (red) is not. It is also seen that the load current (blue) is sinusoidal but with a phase difference relative to $I_{OUT(PA)}$.

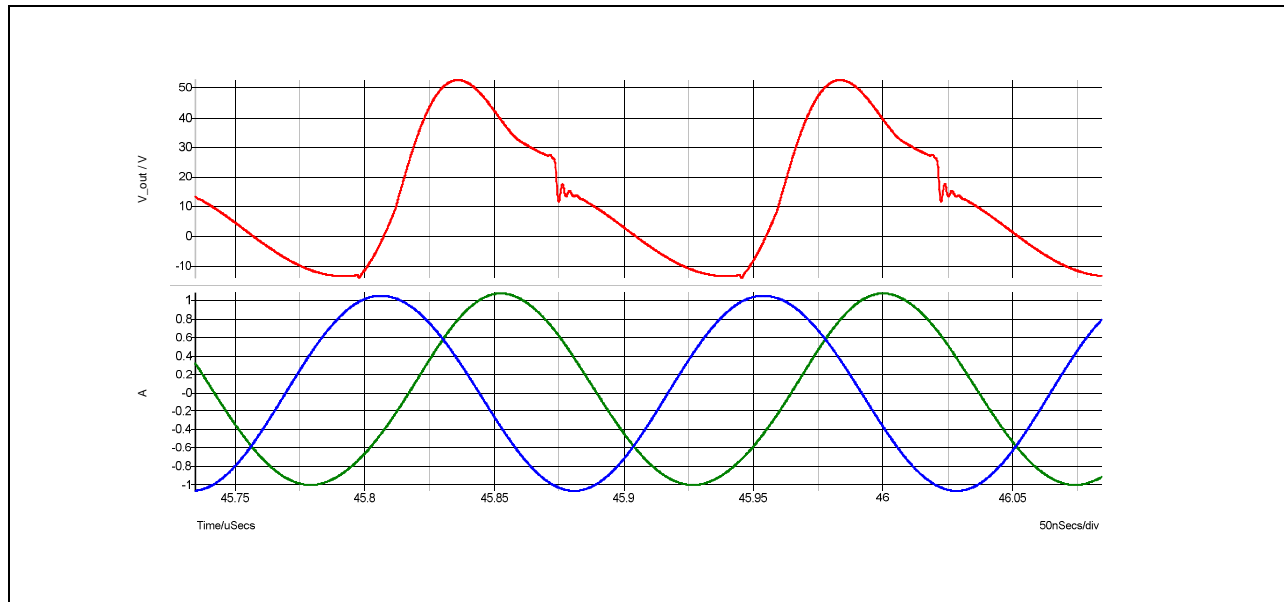


Figure 23 Output waveforms for $k=0.2$

If the coupling factor is reduced to 0.05 the simulated circuit efficiency falls to 45%. This demonstrates that the efficiency is heavily dependent on the distance between the transmit and receive coils.

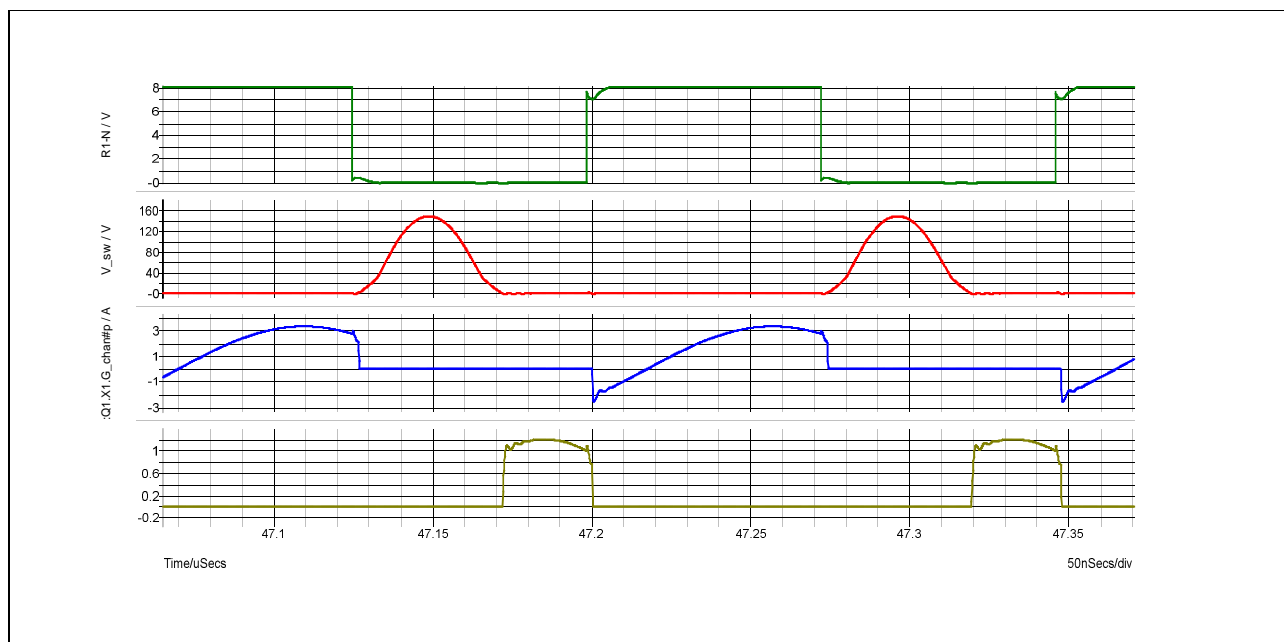


Figure 24 Circuit waveforms for $k=0.05$

Simulated performance

In this case the impedance $Z_{TX_{IN}}$ has changed so that the class-E PA is now operating with R_{LOAD} less than the design point as illustrated in figure 15. The gate drive is shown in green to indicate that the drain voltage now falls to zero some time before the end of the off period. In this case the peak drain voltage (red) is 149V, which is almost 6 times V_{IN} and in addition there is now significant body diode current (yellow). The circuit is however able to operate in this condition since Q1 is rated up to 200V. ZVS is maintained but zero current switching (ZCS) is not. It can be brought back to the design point by increasing the value of C1, in this case to 390pF.

In a real wireless charging system the distance between the transmit and receive coils should not vary greatly, for example the transmit coil is built into a table of specific thickness with devices placed on top that incorporate receive coils. The class-E charger PA component values are then optimized to provide ZVS and ZCS over the desired load range. If necessary a micro-controller can be included in the system to switch in and out capacitors to adjust the operating point as needed according to the ratio of peak drain current to input voltage and/or detection of the drain voltage at the point just before switch on of Q1.

In a practical system would be preferable to use a lower value of L2 to reduce inductor size and losses. The circuit is simulated again with L2 reduced to $1.4\mu H$ and C2 increased to $1nF$. These values give: $f_{r1}=4.25MHz$ and $f_{r2}=10.67MHz$, which fulfil the condition of equation [17]. The condition of equation [18] is also met. The circuit is then simulated for $k=0.1$ over a range of R_{LOAD} from 5 to 25Ω .

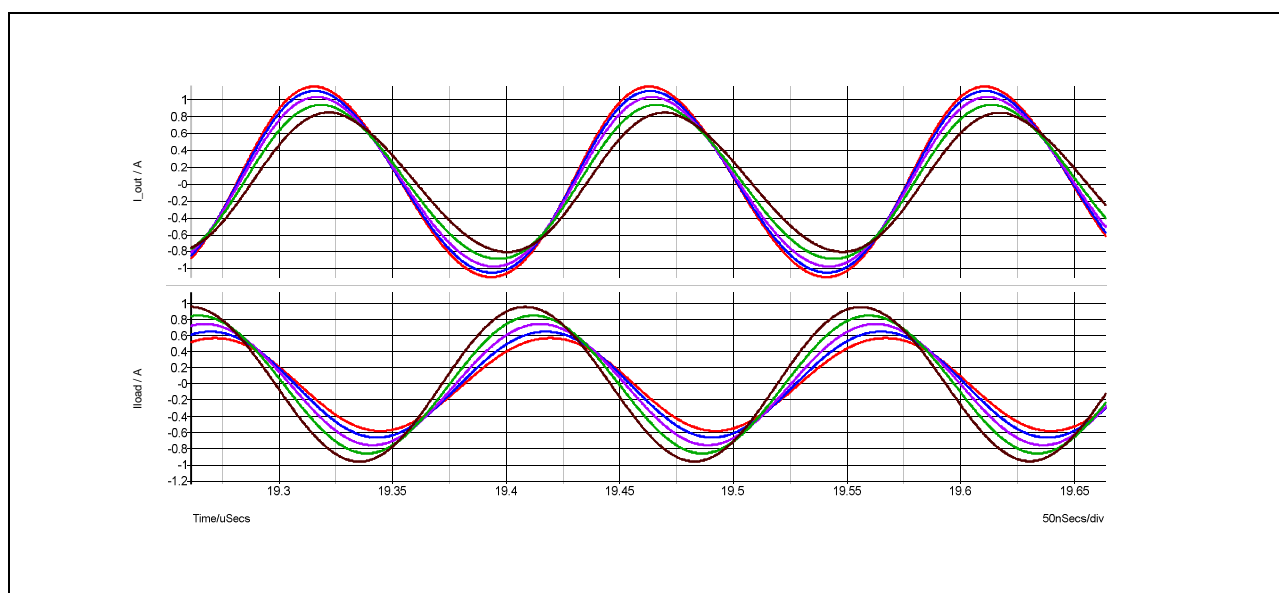


Figure 25 PA output and load current variation with R_{LOAD}

Table 7 Current waveforms for values of R_{LOAD}

R_{LOAD}	Trace color
25Ω	Red
20Ω	Blue
15Ω	Purple
10Ω	Green
5Ω	Brown

Simulated performance

The results show that the output current from the PA reduces as the load resistance is reduced from 25 to 5Ω by about 40% and that the current entering the load increases by about 63%. The power consumed by the circuit falls from 5 to 3.3W and the load power falls from 4.17W to 2.22W. It is seen that for a fixed value of V_{IN} the relationship between the power delivered and load resistance are non-linear.

The following set of results show that both currents are linearly proportional to V_{IN} for a given value of R_{LOAD} :

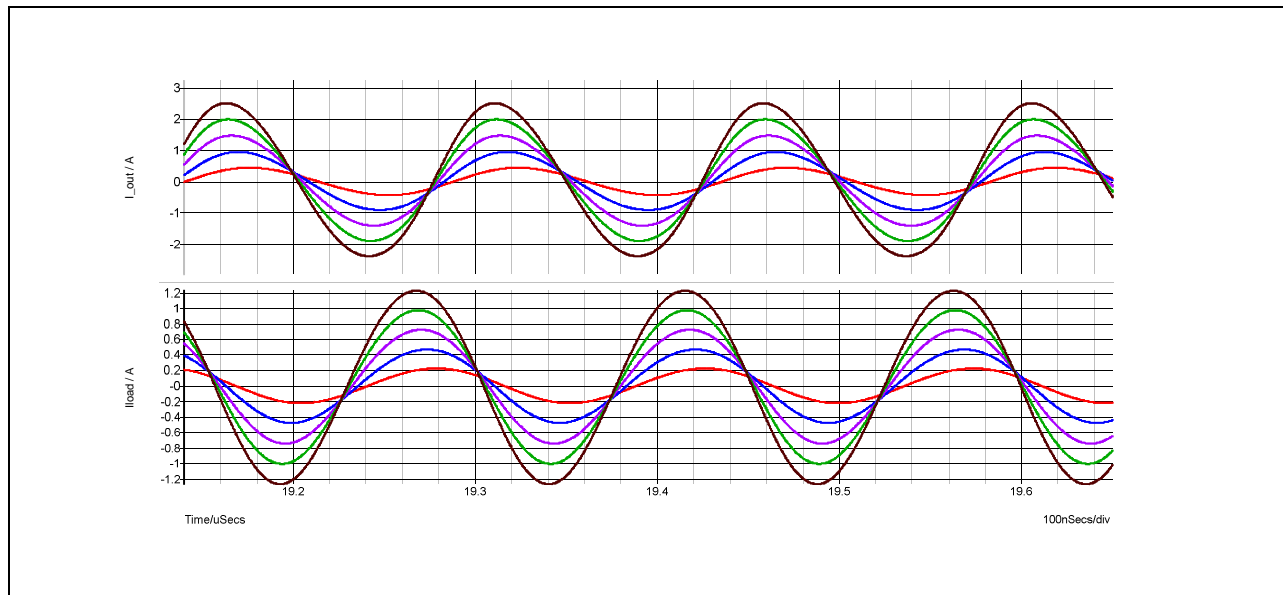


Figure 26 PA output and load current variation with V_{IN}

Table 8 Current waveforms for values of V_{IN}

V_{IN}	Trace color
10V	Red
20V	Blue
30V	Purple
40V	Green
50V	Brown

The set of drain voltage waveforms shown below shows that the peak drain voltage is linearly proportional to V_{IN} and that the period between Q1 switch off and the point at which the voltage falls to zero reduces slightly as V_{IN} increases. This is due to the dependency of C_{oss} on the drain voltage, which means that at lower V_{IN} the average value of C_{oss} over the period is higher affecting the value of f_{r2} . It is seen that ZVS operation is possible over a wide range of V_{IN} except at very low voltage where the amount of hard switching would not cause significant switching losses.

It is noted that FET devices in which the increase in C_{oss} at lower values of V_{DS} is not so great would allow the class-E circuit to operate close to ZVS over a wider range of load.

Simulated performance

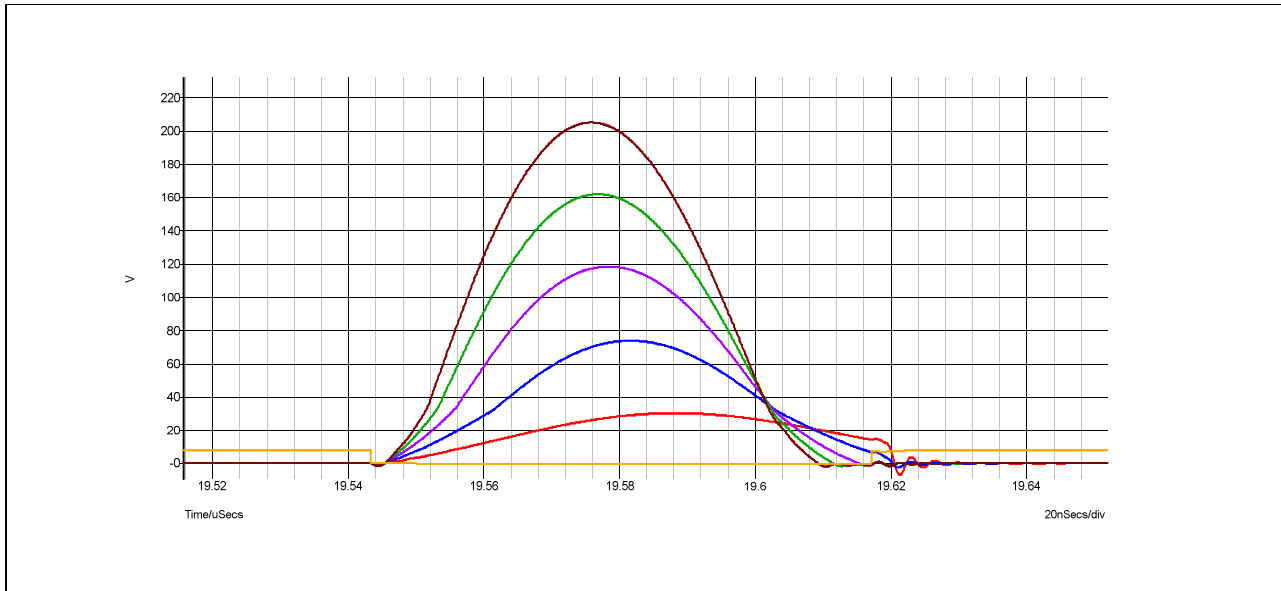


Figure 27 Drain voltage variation with V_{IN}

5 SE class-E evaluation board

5.1 Functional description

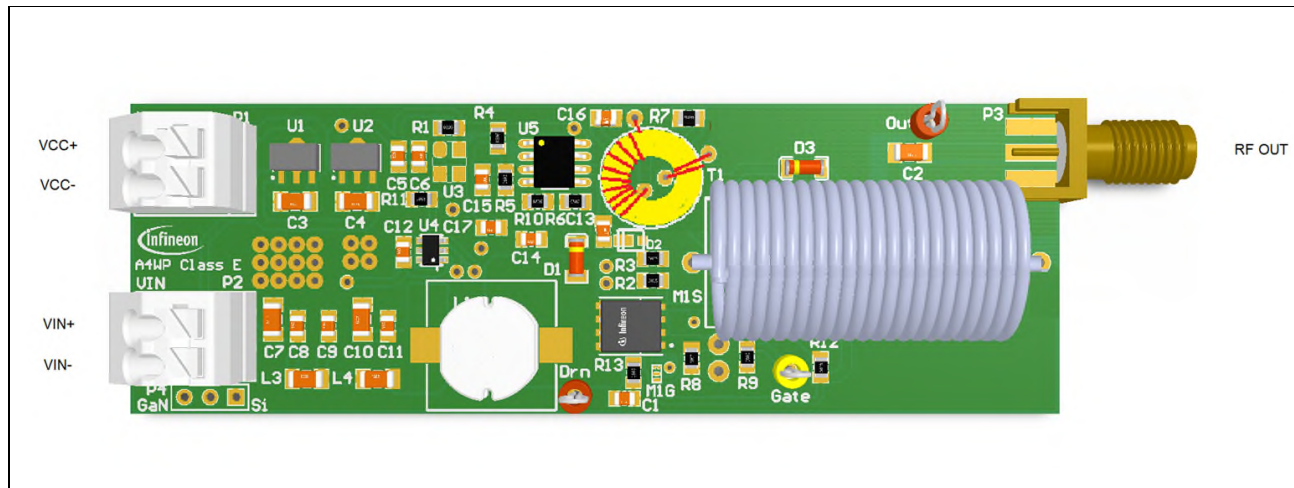


Figure 28 SE Class-E wireless charging evaluation board

The single ended class-E wireless charging evaluation board is able to drive up to 16W load. It has two separate DC power inputs with a common return (VCC- and VIN-). VCC should be connected to a power supply set from 14V to 20V. The internal regulators U1 and U2 provide 12V and 5V rails for the oscillator U3, control circuitry and gate driver U4. VIN should be connected to a variable DC supply up to 50V¹ with current limit set to 0.5A. This powers the RF amplifier section. L2 may be a powdered Iron toroid or air cored RF inductor². As previously discussed the class-E amplifier is only able to operate in ZVS mode with acceptable efficiency³ though this depends heavily on the distance between the coils. It supports a range of loads, where the load is a complex product of transmit and receive coil characteristics, impedance matching components, distance between the coils and the number, type and orientation and charge state of devices being charged.

For evaluation purposes the class-E evaluation board may be operated with a resistive load or suitable transmit resonator such as the Infineon type 1 Air Fuel transmit coil, which is connected through the output SMA connection through a suitable RF cable.

The evaluation board and transmit coil can be used with a suitable receiver coil, rectifier and load. However to operate with Air Fuel compatible portable devices (or devices connected to a wireless charging receiver) Bluetooth communication is necessary to initiate and control power transfer, which the evaluation board does not support.

The evaluation board includes protection circuitry, which causes the power amplifier to enter hiccup mode if any of the following fault conditions occur:

1. The drain peak drain voltage exceeds a limit set below the MOSFET maximum drain-source voltage.
2. The output current exceeds a maximum set limit.
3. The temperature of the copper area around the MOSFET exceeds a threshold of ~100°C.

¹ The input voltage VIN should never exceed 50V.

² An air cored inductor is shown in figure 28.

³ The minimum acceptable efficiency is assumed to be 75%.

SE class-E evaluation board

These protection functions are built around dual open-drain output comparator U5. A reference voltage of approximately 2V formed by the divider consisting of R4 and R5 is used for both comparators. The comparator outputs are connected together and to the output enable (OE) pin of the oscillator U3 operating in conjunction with R1 and C2 to set the restart delay. The output of U3 drives the MOSFET gate through U4. U5A forms the drain over-voltage protection circuit and U5B forms the output over-current protection circuit, sensing the output current through current transformer T1. Temperature is sensed through PTC R13, which forms a divider with R12 to produce a voltage that rises as the temperature increases until it becomes high enough to force U5 pin 6 above the 2V threshold through D3 causing shut down.

IMPORTANT!**Safety Warnings**

To prevent risk of electric shock from RF high voltages the user should avoid touching and part of the system when it is powered. RF electric shock causes burning of skin!

The class-E wireless charger produces high voltages internally and at the output as well as at the transmit coil and its associated components. If a metal variable impedance matching capacitor is fitted, neither this nor any other exposed conductor should be touched during operation.

It is necessary to place an insulator of appropriate thickness between the charging pad and the device(s) being charged!

The power amplifier must always be connected to load such as a resonator or appropriate resistive load board before powering up. Powering into an open circuit will damage the power amplifier!

5.2 Schematic

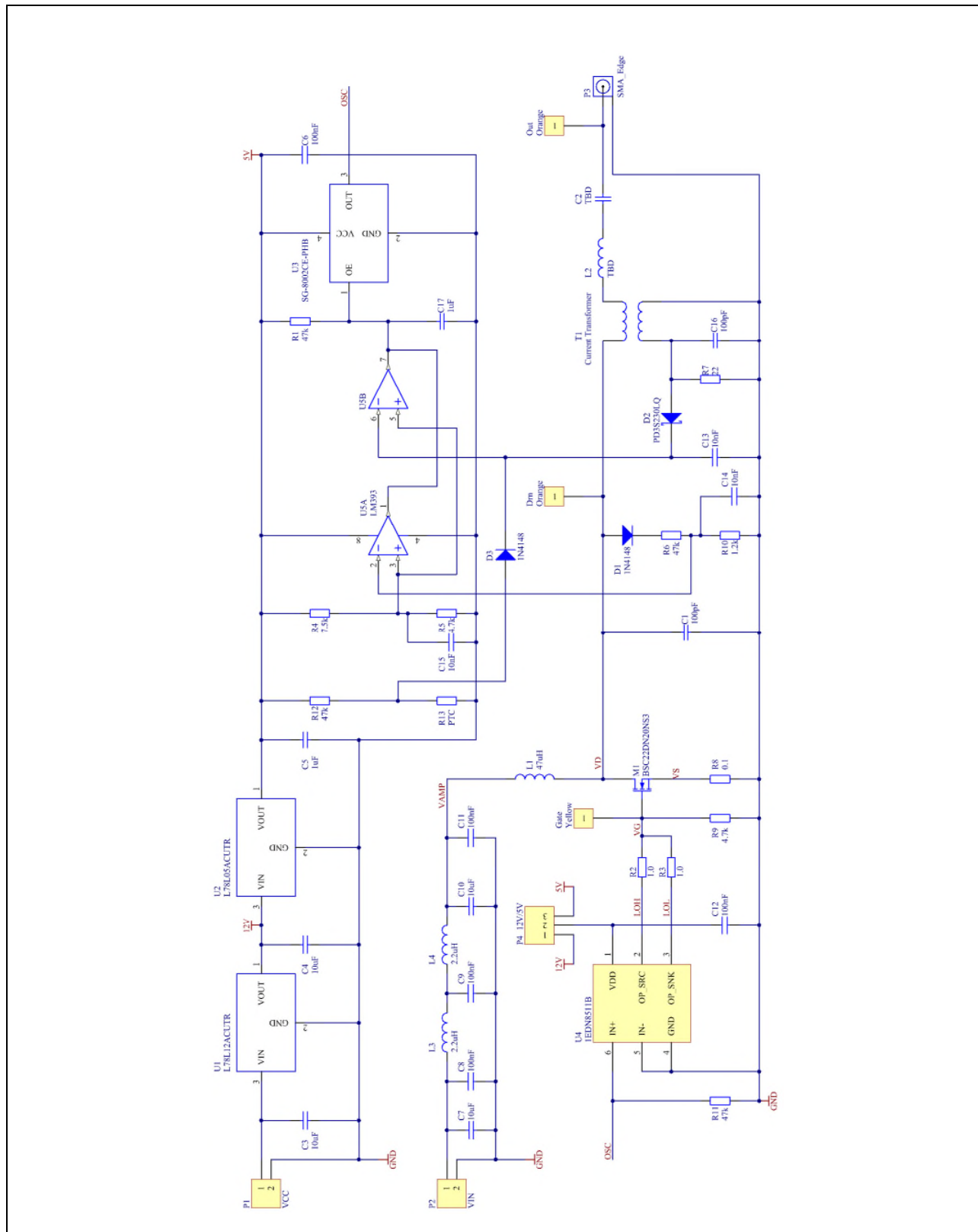


Figure 29 SE class-E evaluation board schematic

5.3 Bill of materials

Designator	Quantity	Manufacturer	Part Number	Value/Rating
C1, C16	2	Wurth	885342207015	100pF/1kV/10%/0805
C5, C17	2	Wurth	885012207051	1uF/16V/0805
C3, C4, C7, C10	4	TDK	C3216X5R1H106K160AB	10uF/50V/1206/10%
C6, C8, C9, C11, C12	5	TDK Wurth	CGA4J2X7R1H104K125AA 885012207098	100nF/50V/0805/10%
C13, C14, C15	3	TDK Wurth	C2012C0G1H103J060AA 885012207092	10nF/50V/0805/10%
C2	1	Wurth	885342008006	1500pF/630V/1206/5% COG/NPO
D1, D3	2	Micro Commercial	DL4148-TP	75V/150mA/MINI MELF
D2	1	Diodes Inc	PD3S230LQ	SCHOTTKY 30V/2A/ POWERDI323
Drain, Out	2	Keystone	5000 series	0.04" dia orange
Gate	1	Keystone	5000 series	0.04" dia yellow
L1	1	TDK	SLF12565T-470M2R4-PF	47uH/2.4A/58mOhm/10%
L2 (option 1)	1		Custom	Air core inductor, 1.5μH
L2 (option 2)	1	Micrometals	T50-6 toroid	16 turns (AWG 22), 1.5μH
L3, L4	2	Murata	LQM31PN2R2M00L	2.2uH/900mA/190mOhm/ 1206
M1	1	Infineon	BSC12DN20NS3	MOSFET N-CH 200V 7A 8TDS0N
P1, P2	1	Wurth	691412120002MB	2 Position 3.5mm
P3	1	Linx Technologies	CONREVSMA013.062	CONN RPSMA PLG STR 50Ohm EDGEMNT

SE class-E evaluation board

R1, R6, R11, R12	4	Panasonic	ERJ-6ENF4702V	47k/0.125W/0805/5%
R2, R3	2	Panasonic	ERJ-6GEY1R0V	1.0/0.125W/0805/1%
R4	1	Panasonic	ERJ-6ENF7501V	7.5k/0.125W/0805/5%
R5, R9	2	Panasonic	ERJ-6ENF4701V	4.7k/0.125W/0805/5%
R7	1	Panasonic	ERJ-6ENF22R0V	22/0.125W/0805/1%
R8	1	Panasonic	ERJ-L06KF10CV	0.1/0.125W/0805/1%
R10	1	Panasonic	ERJ-6ENF1201V	1.2k/0.125W/0805/5%
R13	1	Epcos-TDK	B59721A0100A062	100C/680Ohm at 25C/0805
T1	1	Micrometals	T37-6 toroid	Current transformer, 1:10
U1	1	ST Microelectronics	L78L12ACUTR	IC REG LDO 12V 0.1A SOT89-3
U2	1	ST Microelectronics	L78L05ACUTR	IC REG LDO 5V 0.1A SOT89-3
U3	1	Epson	SG-8002CE-PHB	Oscillator IC
U4	1	Infineon	1EDN8511B	Gate driver IC, 8V, SOT-23-6-2
U5	1	STM	LM393DT	Dual comparator , SO-8

5.4 PCB layout

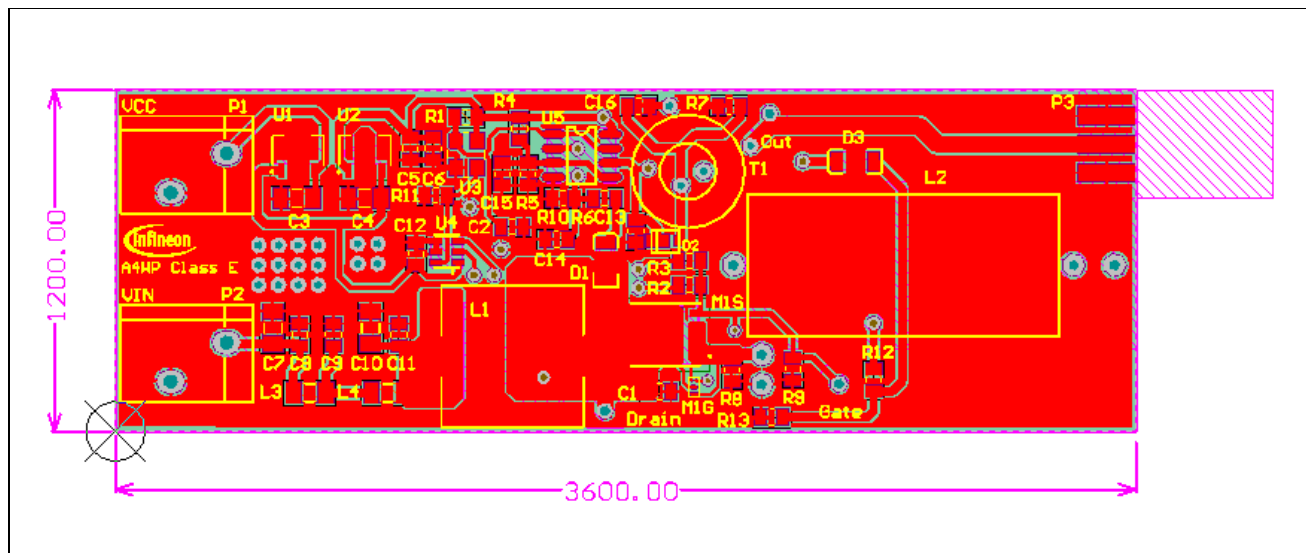


Figure 31 PCB top side

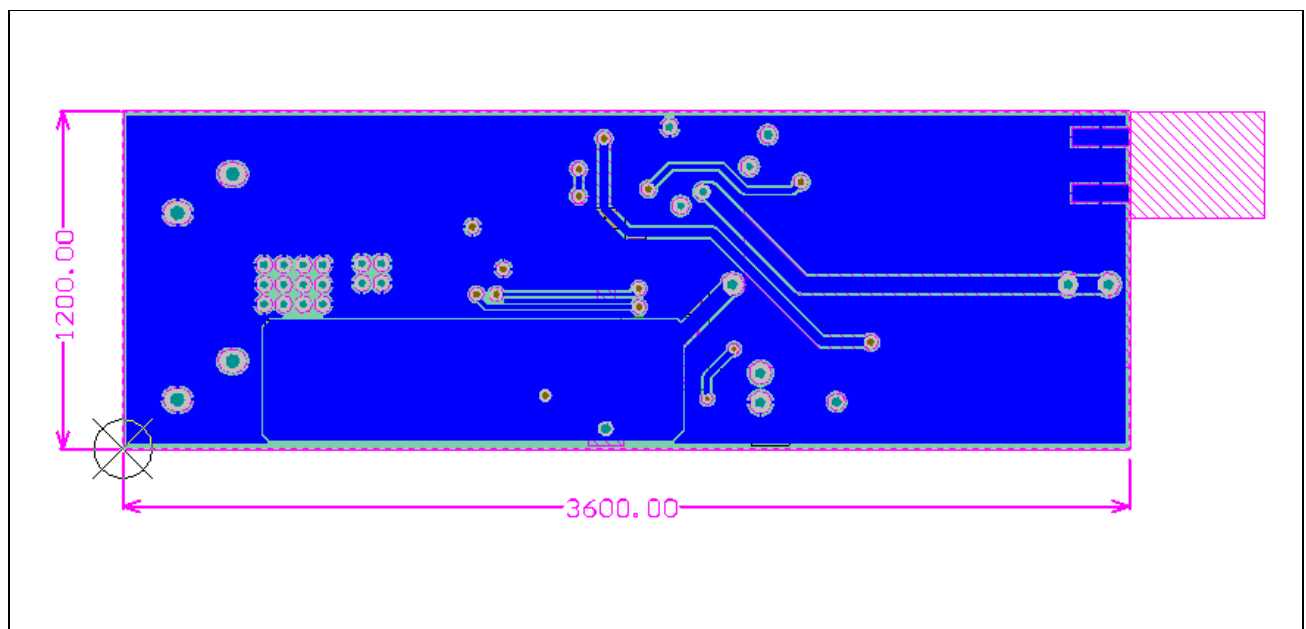


Figure 32 PCB bottom side

In this layout all components are mounted on the top side. The bottom side is composed of a ground plane and a thermal relief plane connected to the MOSFET drain. The wavelength at 6.78MHz is 44.25m, which is much greater than the PCB trace distances on the board so there is no concern about losses due to wave reflection and interference. At this frequency parasitic inductances and capacitances are still small compared to the values of the circuit elements. The output inductor L2 (LP) should be mounted a little above the board to reduce capacitive coupling to the circuit ground.

There is also a ground plane on the top side to reduce unwanted radiated emissions and minimize cross coupling. Signal and power grounds are separated so that high currents can return to the source without passing through the ground connections of sensitive parts of the control circuitry such as the oscillator and protection circuits.

6 RF inductor design

6.1 Output inductor

The choice of output inductor (L_2) depends on the value chosen. Larger values of inductance require larger, more lossy inductors with more turns. As mentioned either a suitable RF Iron powder toroid or an air cored inductor may be used. A wide range of RF toroids are available from suppliers such as Micrometals, which are easier to use since the inductance per number of turns squared is fairly constant. For air cored inductors the value is dependent on length, diameter and spacing between the turns making them more difficult to fabricate. However for higher inductances RF toroidal cores tend to suffer from heating due to core losses so air cored types may be the only viable option.

A single layer air core inductor widely used in RF applications can be designed based on the Wheeler formula:

$$L = \frac{N^2 \cdot d^2}{18d + 40l} \quad [\mu\text{H}] \quad [21]$$

Where N is the number of turns, d is the diameter and l is the core length (both in Inches). The formula is accurate if the turns are touching each other, $d \gg$ the wire diameter and the ratio of diameter to length is less than 3.

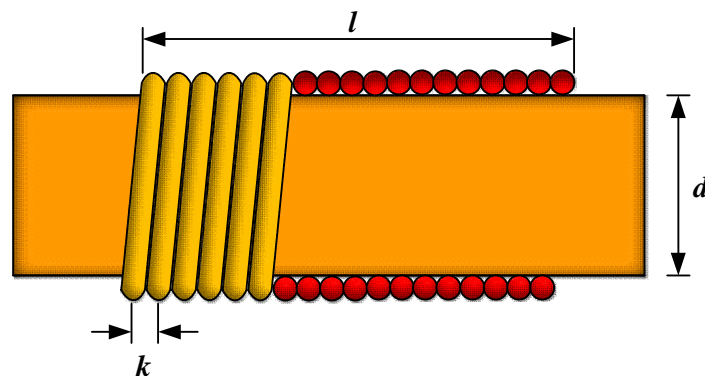


Figure 33 Air core inductor

The following example is wound with AWG22 wire around a 0.5" diameter drill bit held in a vice. The coil is wound tightly so that the turns are touching then cyanoacrylate adhesive is applied to the windings and allowed to dry to hold them together. This is necessary otherwise the turns tend to spring apart altering the inductance.

In this example; $N=27$, $d=0.5$ and $l=0.7$,

$$L = \frac{27^2 \cdot 0.5^2}{(18 \cdot 0.5) + (40 \cdot 0.7)} = 4.93 \mu\text{H}^1$$

¹This is not necessarily a suitable value to use in the application.

6.2 Current transformer

The current transformer is wound on a 10mm diameter Micrometals (T37-6) toroidal core. Iron powder mix number 6 is used, which is specified for operation in the RF range from 3 to 40MHz. The primary is one turn of AWG 22 wire and the secondary is 10 turns of the same size wire. This produces a voltage at R7 proportional to the output current multiplied by the turns ratio multiplied by the resistance. For example for 0.5A a voltage of 1.1V is produced. Since the current transformer is used only to sense the magnitude of the current, the polarity of the windings does not matter.

Transmit coil

7 Transmit coil

The Infineon type 1 transmit coil inductance is approximately $5\mu\text{H}$. It is connected to the class-E PA output through a coaxial cable with SMA connectors. It can be configured to work with single or double ended output power amplifiers by setting the switch (S1) to the “SE” or “DE” position. If the switch is not fitted a jumper can be used at P3 for mode selection. For SE operation the PA should be connected to the main input at P1. P2 is used only for DE operation where two output cables are used. The transmit coil may be pre-tuned with capacitors fitted in some or all of the positions C1 to C4. Alternatively a variable capacitor may be fitted at CV1 to allow manual tuning. If tuning manually the user must monitor the voltage waveform at the drain of Q1 of the class-E PA board paying close attention to the shape of the waveform. If the variable capacitor is not set correctly the impedance will not be matched so the PA will not operate in ZVS mode. This results in hard switching that causes Q1 to heat up quickly, which could result in damage to the PA board. If this does occur it is usually possible to repair the board by replacing Q1.

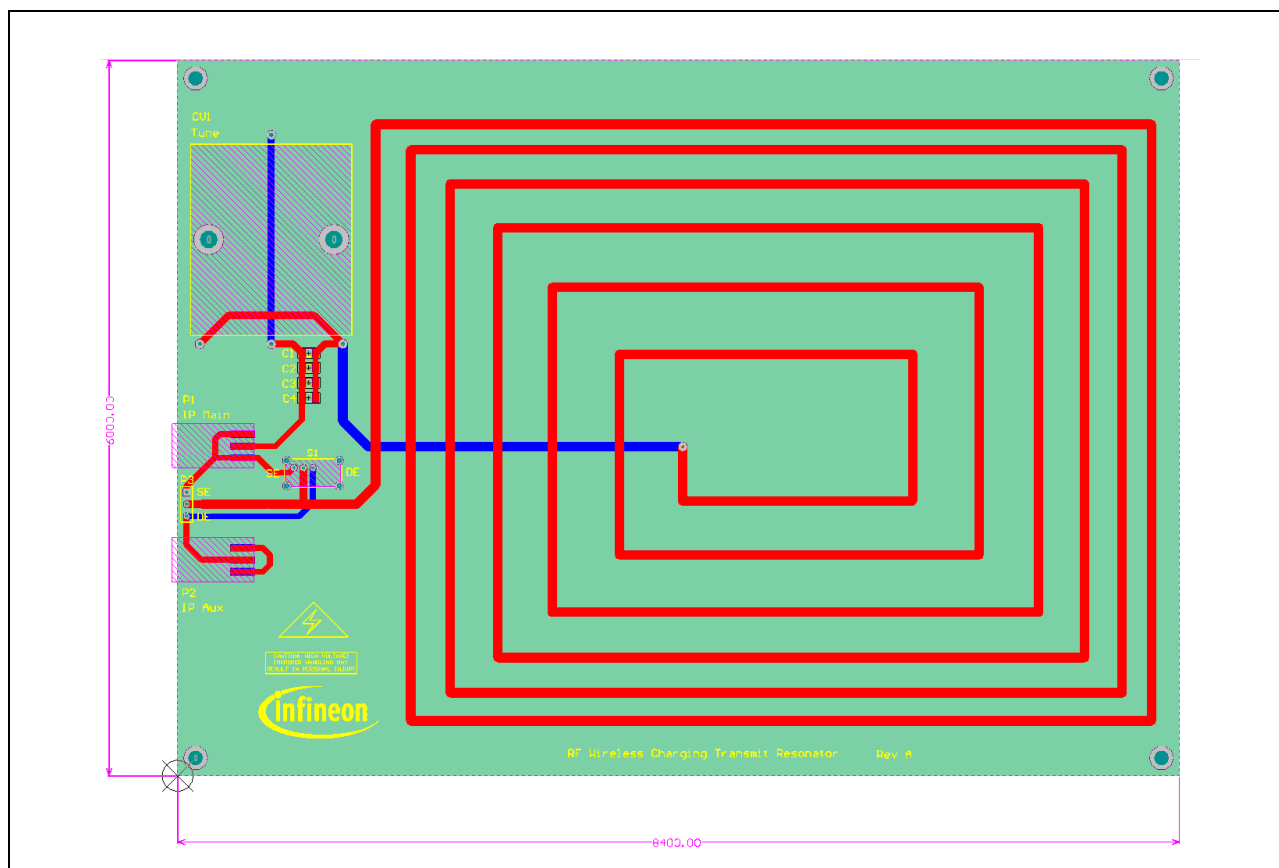


Figure 34 Infineon type 1 transmit resonator board

Safety Warning

The transmit coil board and components also carry RF high voltage during operation. To avoid electric shock or skin burns, exposed conductors should NOT be touched during operation!

The variable capacitor (if fitted) should be adjusted very carefully **using the insulated knob only** and avoiding touching any metal parts.

Test receivers

8 Test receivers

8.1 Resistive load board

The resistor load board shown below can be connected directly to the output of the SE class-E power board for evaluation of the amplifier without coils and impedance matching networks. The load resistance can be set to 25Ω , 15Ω or 5Ω as shown in the table:

Table 9 Current waveforms for values of R_{LOAD}

R_{LOAD}	Switch (1)	Switch (2)
25Ω	Up	Up
15Ω	Down	Up
5Ω	Down	Down

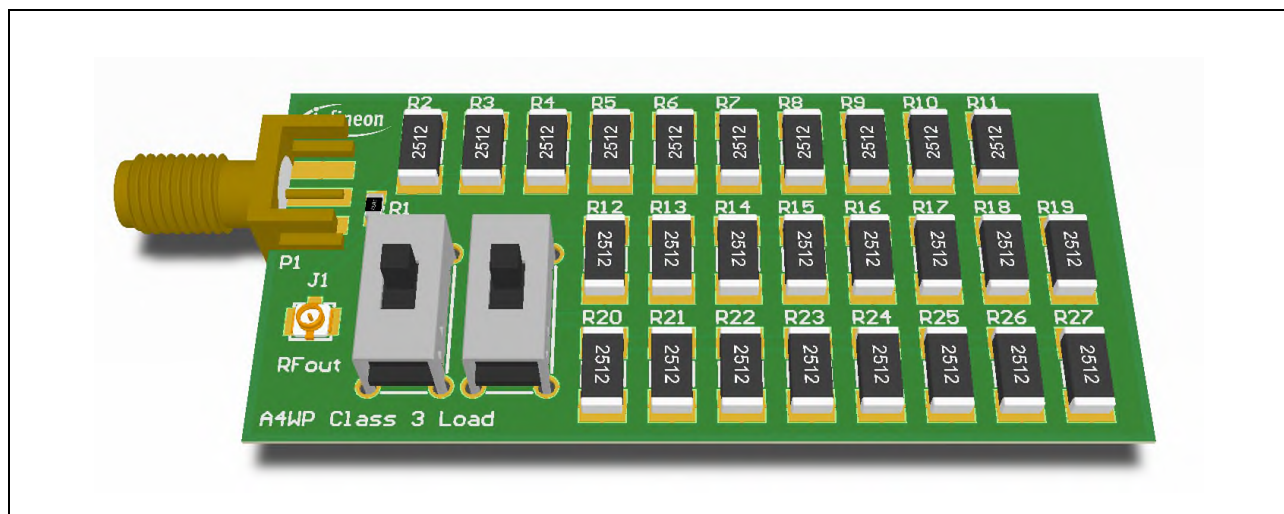


Figure 35 Resistive load board

Safety Warning

The resistor load board can reach very high temperatures with risk of burning if touched and/or damage to the board and class-E board. Care should be taken not to over drive the load board. It is recommended to place a small fan close to the board for forced air cooling.

Test receivers

8.2 Elliptical LED receiver board

The one or more Infineon elliptical LED receiver boards¹ [8] may be used to test the class-E wireless charging evaluation board. When placed on the transmit coil with a distance from 5mm to 25mm it can receive power causing the LEDs to light in sequence. The four LEDs that form the “I” in Infineon indicate the amount of power being received. If all four LEDs are lit green the unit is receiving maximum power. If all four LEDs turn red this is a warning that too much power is being received, which risks damaging the board.



Figure 36 6.78MHz LED receiver board (Air Fuel)

8.3 Receiver load board

The receiver load board includes a bridge rectifier and smoothing capacitor to produce a DC voltage between VOUT and COM when the coil is placed on top the transmitting coil. A load **of up to 1A** can be connected to the LOAD+ and LOAD- terminals with an ammeter connected from IOUT+ and IOUT- (or these may be bypassed). Care should be taken not to overload the board as this may result in damage.



Figure 37 6.78MHz receiver load board (Air Fuel)

¹ Designed by Management Center Innsbruck University (Austria)

Test receivers

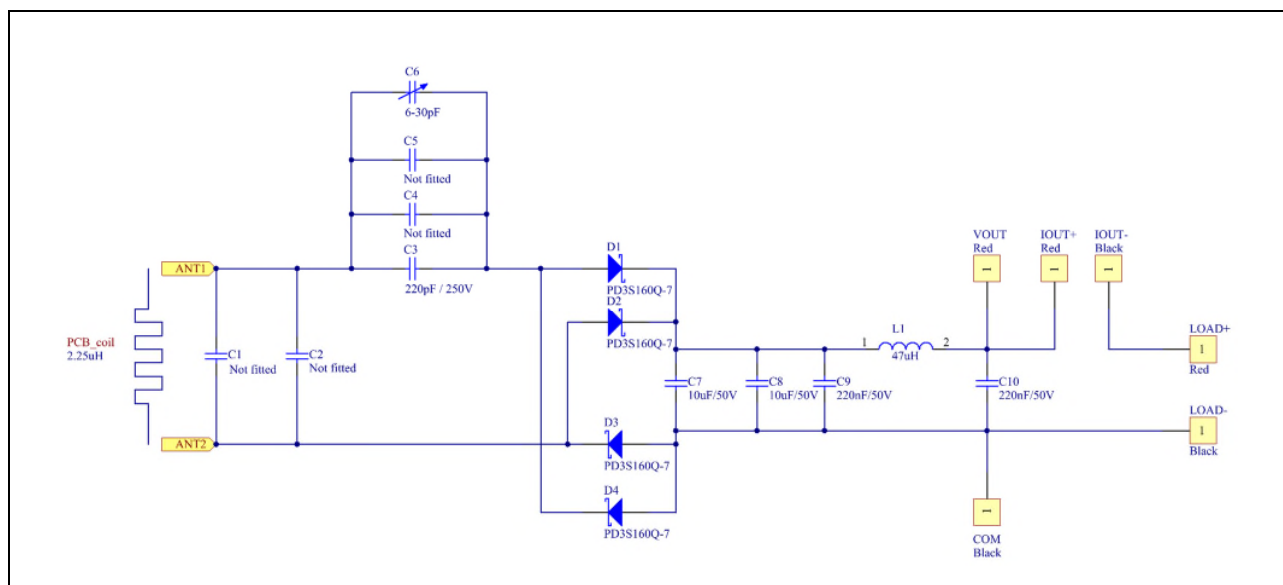


Figure 38 6.78MHz receiver load board (Air Fuel) schematic

The receiver load board uses a $2.25\mu\text{H}$ spiral PRU coil formed from a Copper trace as part of the board as in the elliptical LED board. In the same way it is connected through impedance matching capacitors to a bridge rectifier consisting of Schottky diodes followed by smoothing capacitors with a DC filter to remove HF ripple from the output. The board can be optimized by changing C3 and/or adding parallel capacitors in positions C1 and C2 or additional series capacitors in positions C4 and C5. By adjusting these values the receiver can be tuned to resonance to provide the system maximum efficiency under a particular load condition.

The board includes test point to add voltage and current meters at the DC side with additional connections for an electronic load. Since the DC output voltage varies considerably depending on load receivers included in most practical devices include a buck regulator stage to provide constant output voltage.

As with the elliptical LED board the receiver load board can be damaged by placing it in too strong an oscillating magnetic field. By doing so the diode reverse breakdown voltage could be exceeded. Care should be taken to avoid doing this.

Test results

9 Test results

The PA board was fitted with a $1.5\mu\text{H}$ inductor using a Micrometals T37-6 toroid with 22 turns of AWG 30 wire for L2, a 100pF capacitor for C1 and 1nF for C2. COSS is typically 39pF for the BSC12DN200NS3 yielding an fr1 of 4.11MHz and fr2 of 11.76MHz .

9.1 Resistive load board tests

The resistive load board was connected directly to the PA output with no coaxial cable. The input voltage was adjusted to provide 16W power to the 25Ω and 15Ω loads and as much power as possible to the 5Ω load before exceeding the maximum drain voltage limit of 200V.

Table 10 Resistive load test results

R _{LOAD}	V _{LOAD(RMS)}	P _{OUT}	V _{IN}	I _{IN}	P _{IN}	P _{AUX}	Efficiency	V _{DS(PK)}	V _{DS(PK)/V_{IN}}
[Ω]	[V]	[W]	[V]	[A]	[W]	[W]		[V]	
24.7	19.8	15.87	31	0.55	17.05	0.28	91.6%	113	3.65
15.3	15.6	15.91	35	0.49	17.15	0.28	91.3%	140	4.00
5.5	8.2	12.23	45	0.29	13.05	0.28	91.7%	200	4.44

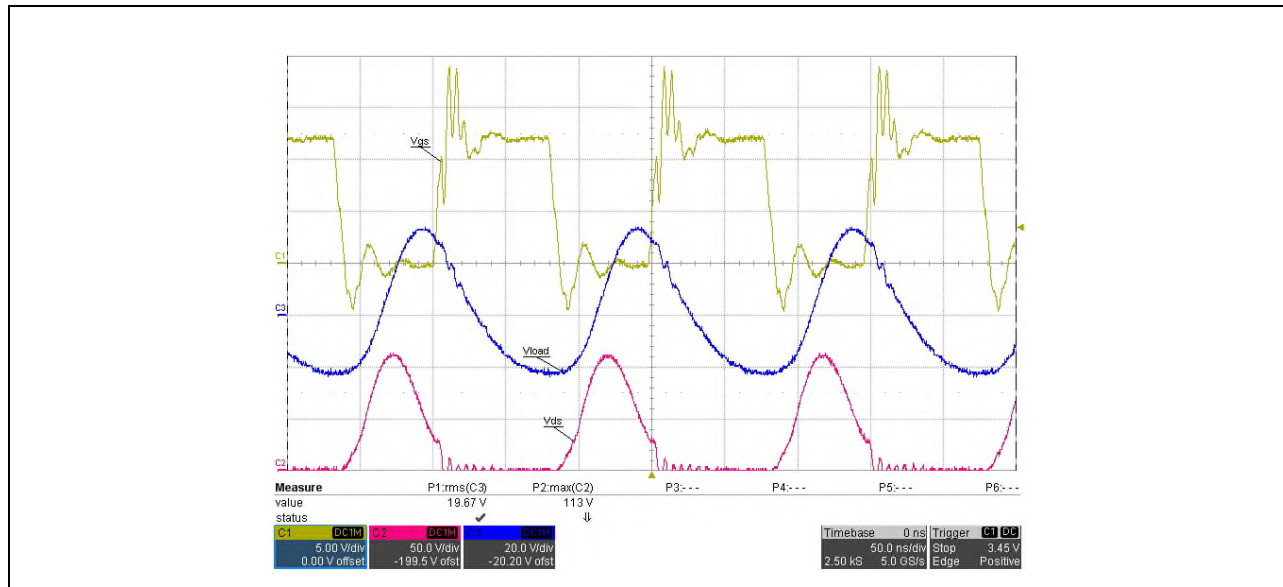


Figure 39 25Ω resistive load waveforms

V_{GS} (yellow), V_{DS} (red), V_{LOAD} (green)

Test results

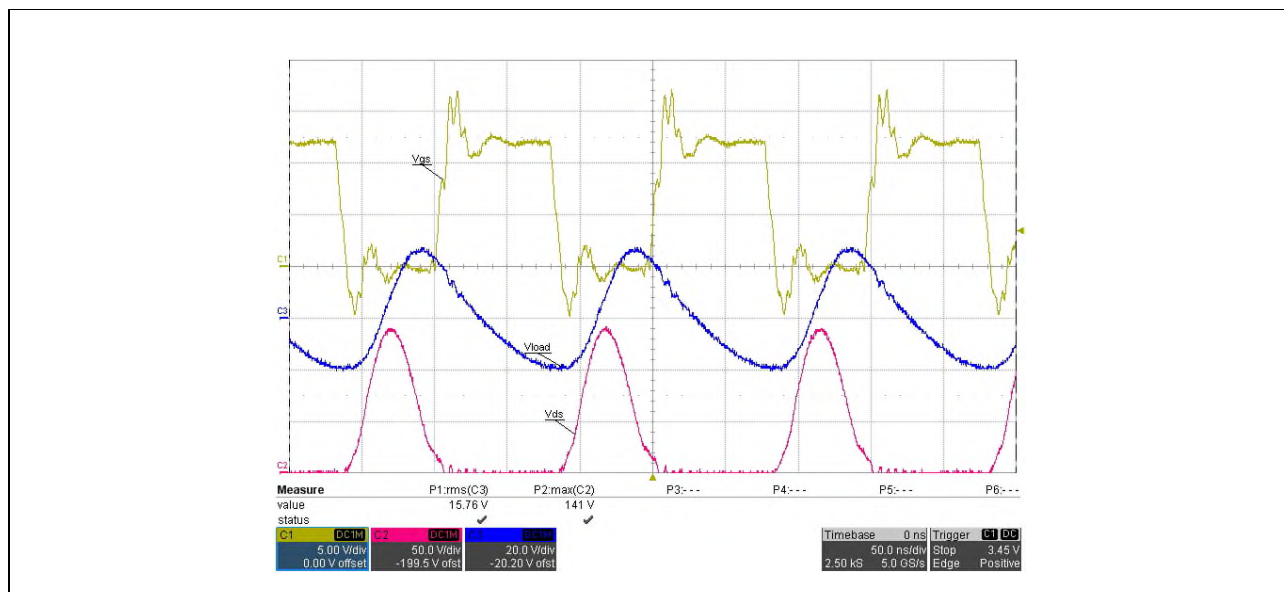


Figure 40 15Ω resistive load waveforms
V_{GS} (yellow), V_{DS} (red), V_{LOAD} (green)

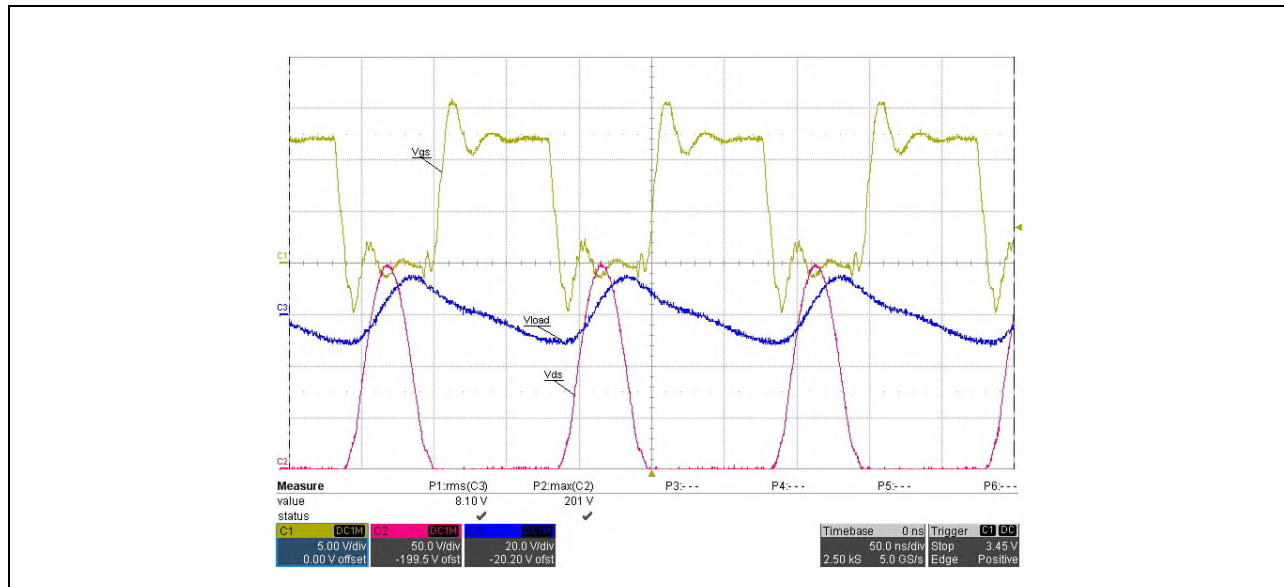


Figure 41 5Ω resistive load waveforms
V_{GS} (yellow), V_{DS} (red), V_{LOAD} (green)

Test results indicate that PA efficiency remains above 90% even though under heavier loads the class-E circuit moves away from the operating point resulting in a higher peak drain voltage. This limits the operating range without having additional C1 added to the circuit to maintain the operating point under such load conditions.

Test results

9.2 LED load board tests

The class-E PA was connected to the transmit coil through a coaxial cable with the impedance matching series capacitor adjusted for ZVS operation (measured at 86pF). The board was powered up with V_{IN} set to 24V without any receiver placed on the transmit coil. In this case the input current I_{IN} is measured at 0.26A, which indicates that during this idling state some power is being consumed by the various elements of the circuit and PTU.

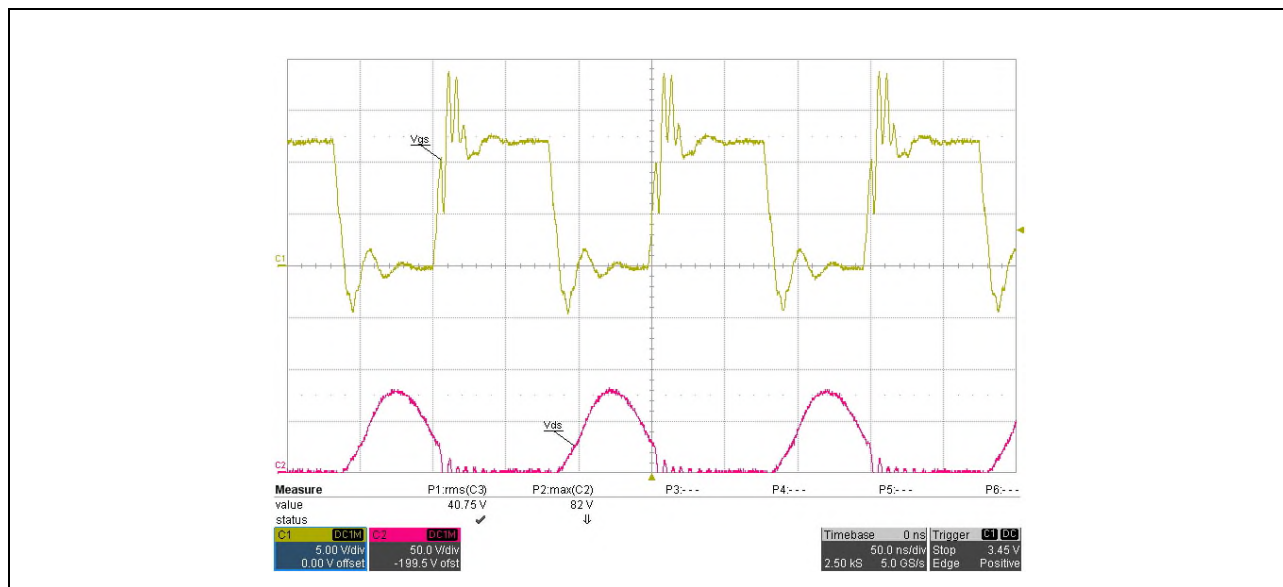


Figure 42 Transmit coil with no receivers placed

V_{GS} (yellow), V_{DS} (red)

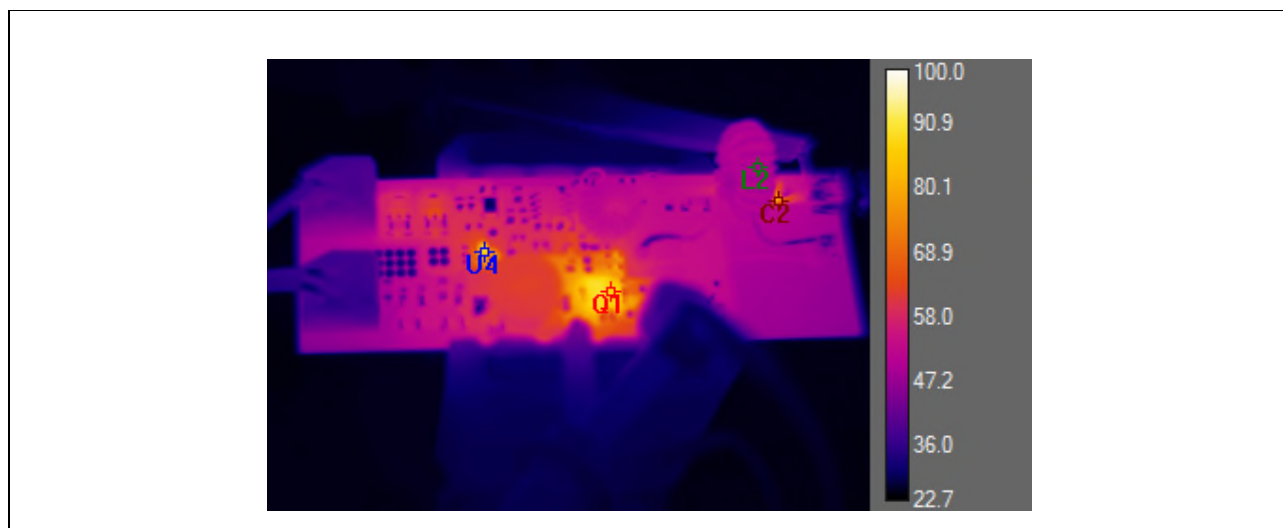


Figure 43 Thermal image of PA in idle mode

It is seen here that Q1 accounts for most of the losses in the PA but that the temperature rise remains within acceptable limits indicating that most of the power consumed is not being dissipated here. This conclusion is backed up by the previous test results that show power loss of typically 1.5W in the PA. The remaining power loss may be accounted for in the oscillating magnetic field being generated. To avoid power wastage in a full wireless charging system the transmitter would need to be shut down until the presence of a receiver is either detected or signaled through some form of communication such as Bluetooth.

Test results

An LED receiver board is now placed on the transmitter at the center with 16mm spacing. The input current to the PA (I_{IN}) now increases to 0.33A:

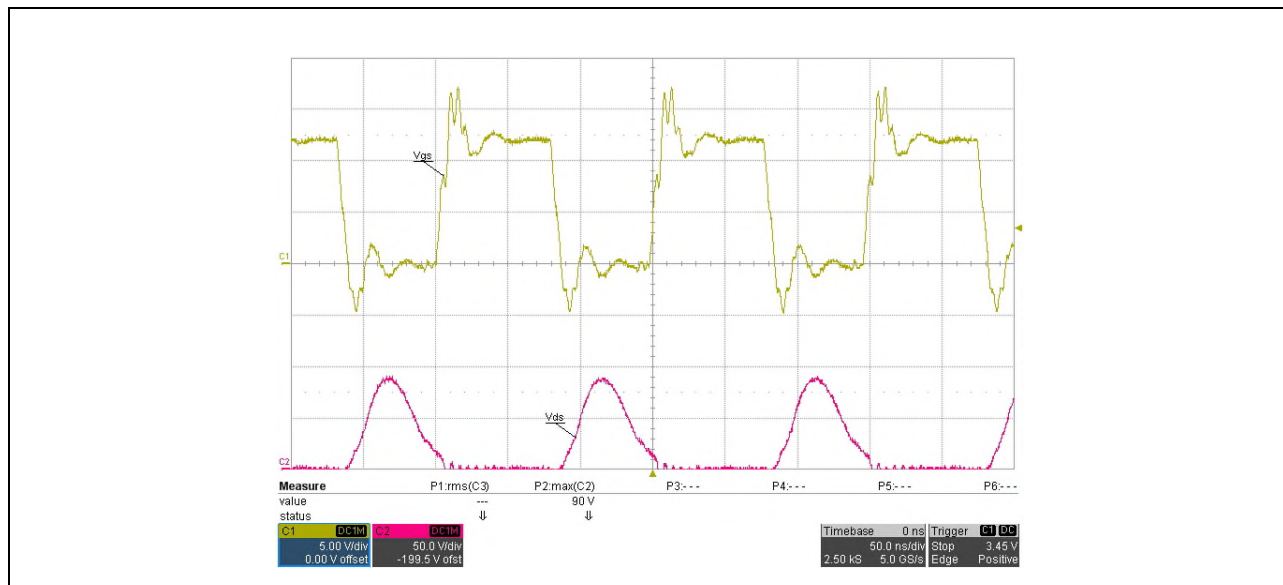


Figure 44 Transmit coil with one LED receiver placed
 V_{GS} (yellow), V_{DS} (red)

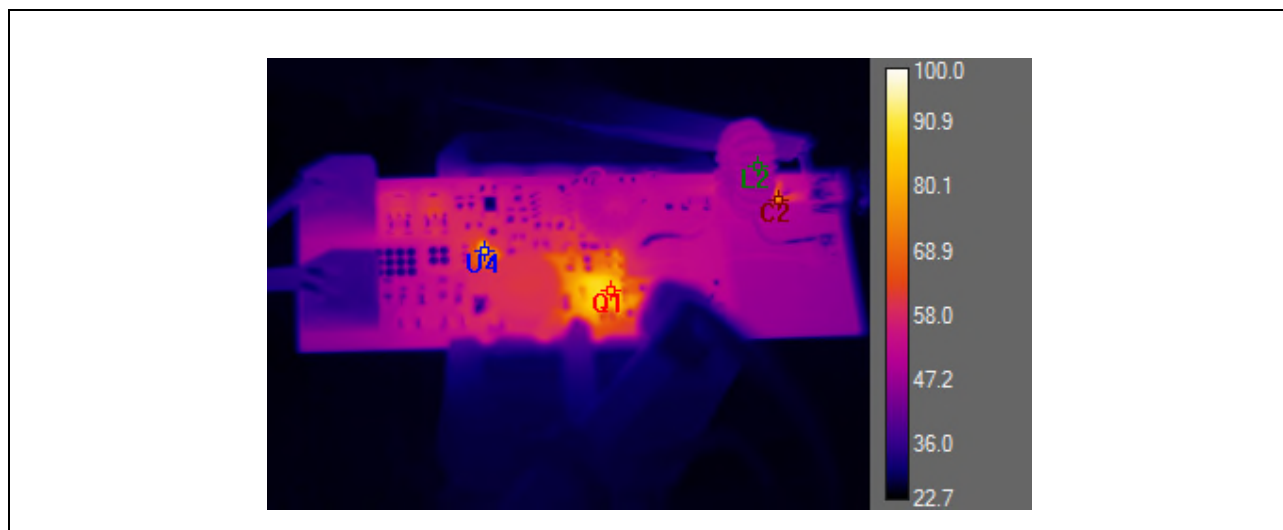


Figure 45 Thermal image of PA powering one LED receiver

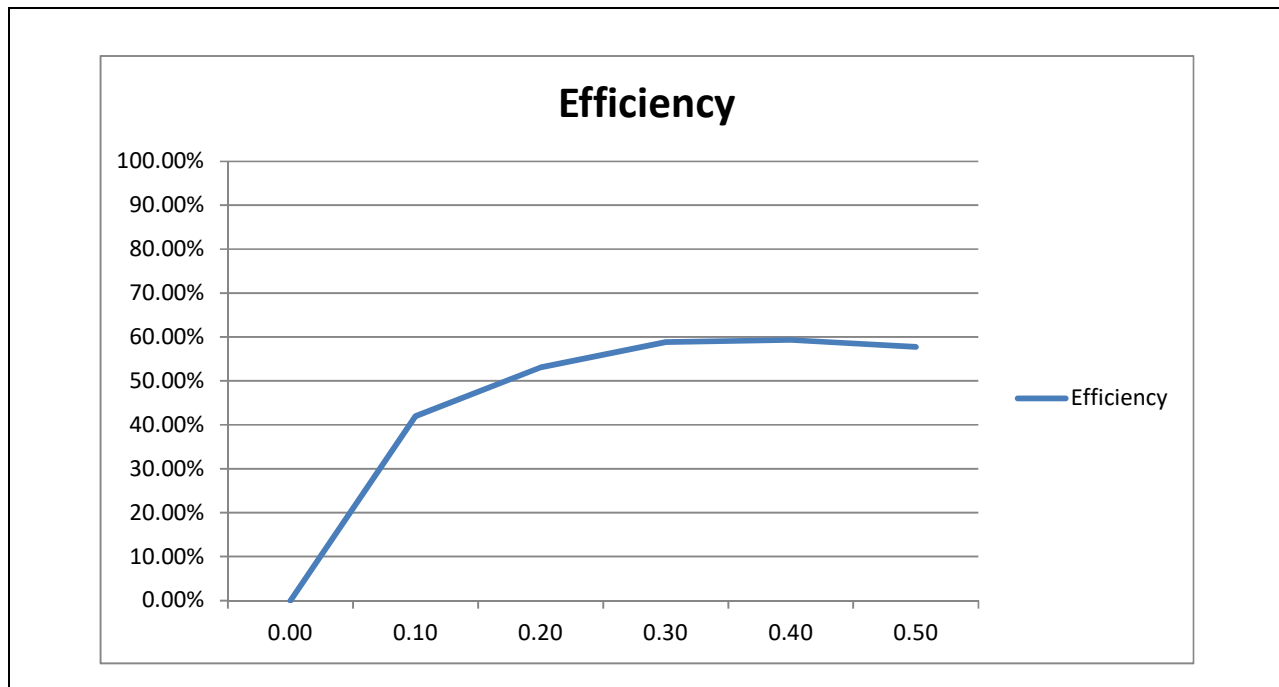
The LED board consumes approximately 4W with the four power level indicator LEDs lit green. It can be seen that the operating point has not shifted reducing the amount of hard switching. There is no appreciable change in the component temperatures suggesting that power previously being wasted is now being transferred to the load.

Test results**9.3 Receiver load board tests**

Tests were carried out using the receiver load board connected to an electronic load and mounted at a distance of 12mm from the transmit coil. For this test the transmit coil fitted with a variable tuning capacitor is used, which is adjusted to give the best possible drain voltage at Q1 as the load is adjusted. The electronic load is set to constant current mode at measured at 0.1A intervals.

Table 11 Resistive load board test results

I _{LOAD}	V _{LOAD}	P _{OUT}	V _{IN}	I _{IN}	P _{IN}	C _{TUNE}	Efficiency	V _{DS(PK)}	V _{DS(PK)/V_{IN}}
[Adc]	[V]	[W]	[V]	[A]	[W]	[pF]	[%]	[V]	
0	60.0	0	24	0.26	6.24	90.0	0	97	4.04
0.1	34.3	3.43	24	0.34	8.16	90.6	42.0	92	3.83
0.2	30.6	6.12	24	0.48	11.52	90.6	53.1	87	3.63
0.3	29.2	8.76	24	0.62	14.88	88.9	58.9	83	3.46
0.4	26.7	10.68	24	0.75	18.00	84.8	59.3	78	3.25
0.5	23.3	11.65	24	0.84	20.16	81.8	57.8	82	2.92

**Figure 46 Efficiency vs load current**

In this case the maximum overall system efficiency reached in this basic test setup is just under 60%. It is seen that although the class-E power amplifier is over 90% efficient when tuned to the optimum ZVS operating point and driving a purely resistive load, additional losses occur when transferring power from the PTU to the PRU. This is partly due to the low coupling factor 'k' and the distortion effect of the bridge rectifier and smoothing capacitor in the receiver. There are also resistive losses in the resonators and connecting cable that limit the Q of each resonator.

Test results

Further system optimization is needed to meet Air Fuel class 3 targets. This would include: optimization of inductors, direct connection of the transmit coil to the PTU, optimization of transmit and receive resonator coil designs and the inclusion of a Buck regulator in the receiver to provide a regulated output and avoid drawing a high current from the rectifier.

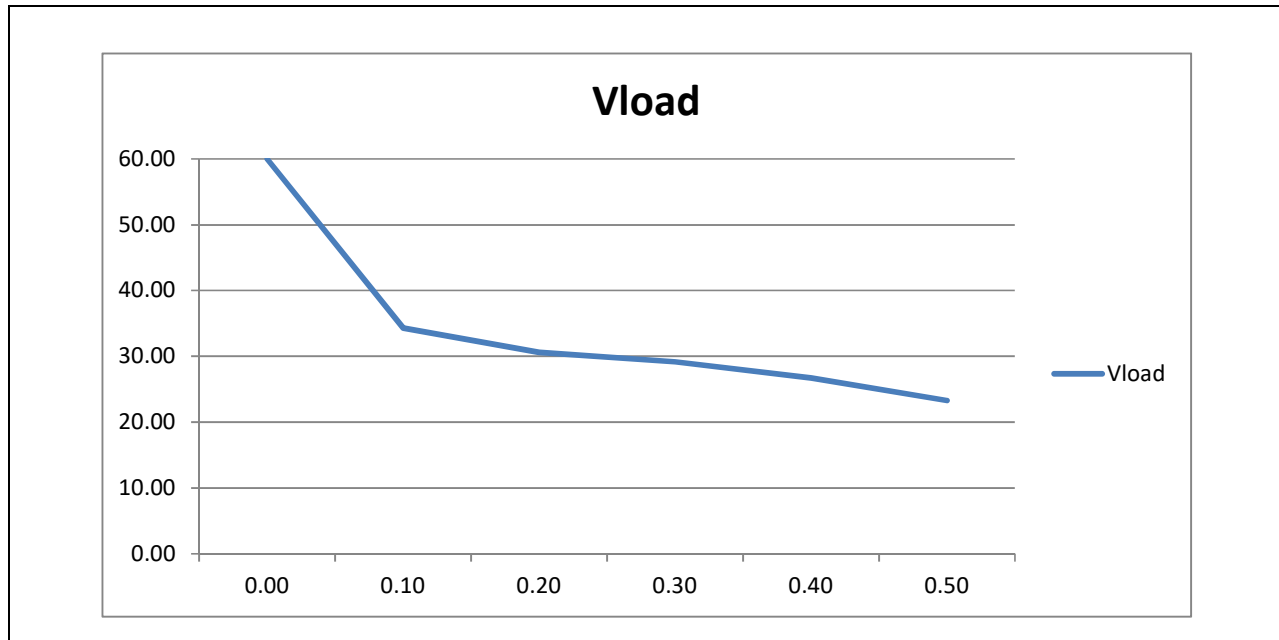


Figure 47 Output voltage-current characteristic

The open circuit output voltage is 60V, which drops significantly when load is applied. Between 0.1A and 0.5A the voltage falls roughly linearly as current is increased. The effect of increasing the load on the drain voltage waveform of Q1 is shown in the following waveforms:

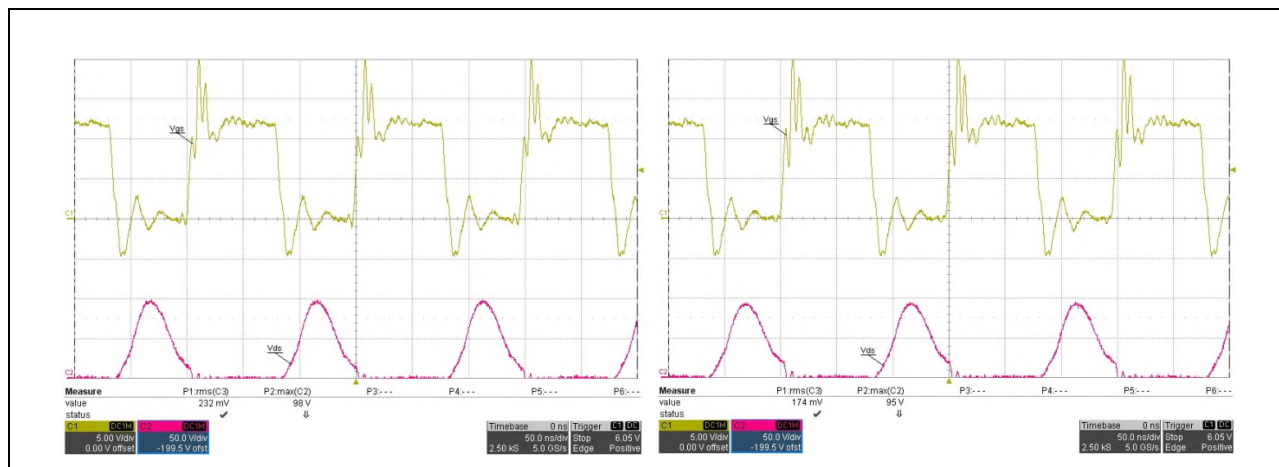


Figure 48 Q1 drain voltage at zero load current (left) and 0.1A load current (right)

Test results

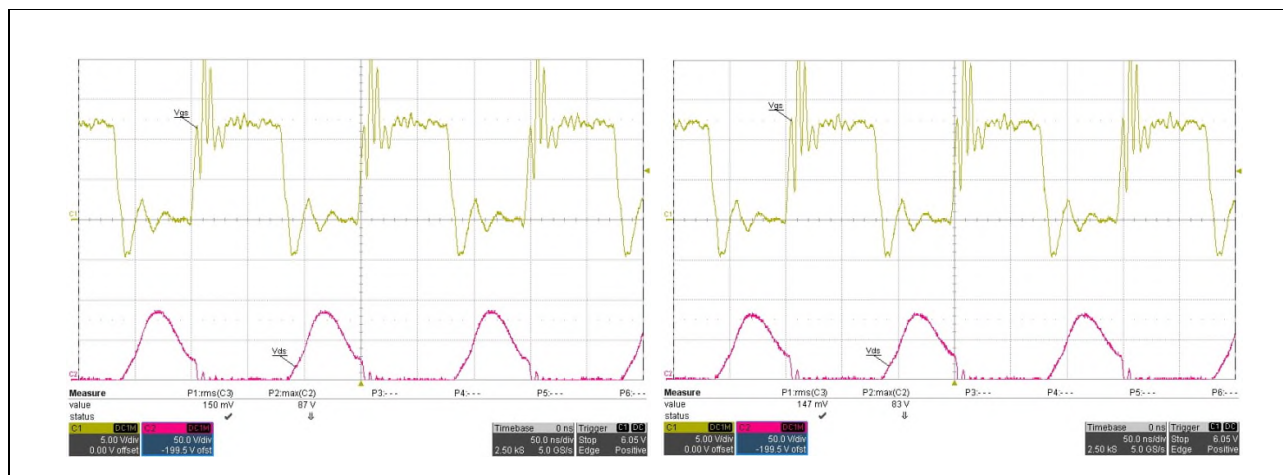


Figure 49 Q1 drain voltage at 0.2A load current (left) and 0.3A load current (right)

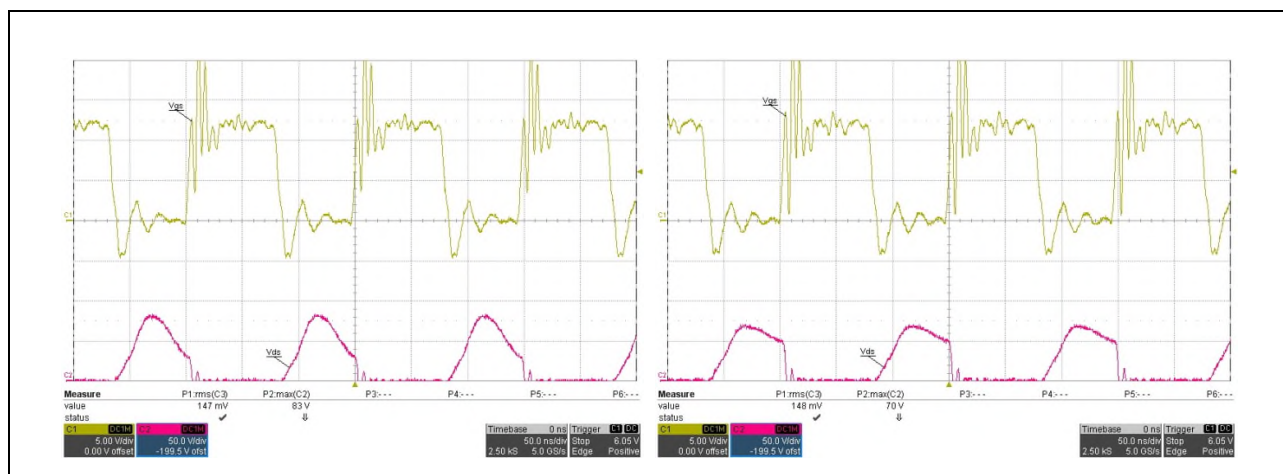


Figure 50 Q1 drain voltage at 0.4A load current (left) and 0.5A load current (right)

The effects of increasing the load are seen in the form of a gradual increase in hard switching, which cannot be eliminated by adjusting the value of the series tuning capacitor in the receiver. This becomes severe at 0.5A.

Conclusion

10 Conclusion

It has been shown that selection of the MOSFET Q1 as well as the passive components C1, C2 and L1 and L2 are very critical to obtain correct operation of the class-E power amplifier. The circuit has two resonant frequencies depending on whether Q1 is in the on state or off state. A method has been given for calculating these resonant frequencies and combining the results to determine a set of values that will exhibit the desired ZVS operation. The procedure developed by N. Sokal for fine tuning the values for optimum results is also included. C1 and C2 should be NPO/COG types for stability at high frequency and low losses. An off the shelf ferrite inductor may be used for L1, however L2 requires a core material suitable for RF operation such as an Iron powder toroid or an air cored inductor. To avoid overheating of L2 and/or C2 their values should be selected for low impedance, therefore lower inductance for L2 and higher capacitance for C2. Although higher values of L2 and lower values of C2 would allow the class-E circuit to operate with ZVS as long as the conditions described in the design equations are met, it is important keep in mind that the output current passes through both of these components resulting in power losses. These are due to skin effect and core loss in L2 and the combined effects of ESR, ESL plus dielectric and other losses related to the structure of the electrodes and dielectric in C2. It is also possible to significantly reduce the physical size of L2 by selecting a lower inductance. It is also necessary to consider the high RF voltages present across L2 and C2 in the resonant circuit. Components need to be rated to withstand such voltages. There is also significant risk of electric shock if the user comes into contact with the circuit.

A MOSFET with $V_{DSS(BR)}$ of at least 200V is required for a single ended Air Fuel class-E class 3 (16W) power amplifier to be able to drive loads in the 5 to 25Ω range. Since the input voltage cannot exceed 50V the power into a 5Ω load is limited to a value below 16W. 150V MOSFETs could be sufficient for low power class 1 and class 2 applications or dual switch differential class 3 designs where the output power is four times that for a single ended circuit with the same input voltage and load.

The results clearly illustrate that C_{oss} is the most critical limiting factor to realize ZVS operation. Hard switching is difficult to eliminate completely because of the large increase in C_{oss} at lower drain-source voltages. However the hard switching step voltage can be limited to below 20V over a useful load range when using the BSC12DN20NS3 OptiMOS 3 MOSFET. This limits losses and temperature rise to an acceptable level. With a small amount of hard switching it is still possible to achieve acceptable efficiency.

Next generation silicon and gallium nitride transistors exhibit a lower and flatter C_{oss} vs V_{ds} characteristic, which can further improve the efficiency the class-E power amplifier and also maintain ZVS operation over a wider output impedance range.

It should be emphasized that operating the class-E amplifier with no load connected or with incorrect circuit values results in severe hard switching and rapid temperature rise. Considering the high switching frequency of 6.78MHz used in resonant wireless charging, care must be taken to avoid this from happening otherwise the MOSFET will rapidly overheat causing failure.

The efficiency of the single ended class-E power amplifier exceeds 90% under optimum ZVS conditions however in a complete system there are additional losses due to the limited Q factors in the two resonators combined with impedance and distortion effects that prevent ZVS operation. It also is seen that efficiency reduces with increasing distance between the resonator coils as the coupling factor 'k' reduces. However it is important to remember that placing the coils too close together can cause overloading of the receiving devices therefore transmission power needs to be controlled in a real system to avoid component damage.

In a full Air Fuel system the values of C1 and C2 could be adjusted by switching different binary weighted capacitors in and out of the circuit to track the operating point. A micro-controller such as the XMC series could be used to sense the peak drain voltage and the phase difference between the output current with respect to the gate drive and possibly also the voltage level at the switch on point of Q1 and use this information to make

Conclusion

adjustments to C1 and C2. The same micro-controller would also be used to control a pre-regulator to supply the input voltage to the power amplifier which can be set according to the requirements of the devices placed on the charging pad. In addition it is necessary to add protection features as included in the evaluation board, which disable the gate drive if the peak drain voltage or the output current gets too high. These protections would typically operate in hiccup mode so that the system would revert to normal operation automatically once the fault condition has been removed.

The receiver bridge rectifier and smoothing capacitor creates a distortion effect on the class-E power amplifier drain voltage that results in hard switching. This effect becomes more severe as load current is increased. To reduce this effect and to produce a regulated voltage output, the receiver in a practical system includes a buck regulator stage such as that included in the elliptical LED receiver board.

Detailed simulations are demonstrated in this application note as a very useful design aid and means of gaining detailed understanding of how the circuit functions. An evaluation kit has been developed consisting of a single ended class-E power amplifier board based on the BSC12DN20NS3 MOSFET and 1EDN8511 gate driver IC combined with an Infineon type 1 transmit resonator to demonstrate real world performance. Test results and waveforms have been presented for different load conditions.

Since the peak drain voltage approaches 200V under some load conditions with input voltage at the 50V limit, it is clear that for power amplifiers to deliver outputs above 16W (class 3) it would be necessary to use the double-ended differential class-E topology. Since the differential circuit is able to supply four times as much power into the given load impedance at a given input voltage this enables systems up to 70W to be realized.

Designers not already experienced with the class-E power amplifier are advised to use simulations to gain a firm understanding of the circuit and the effects of different component value selections and line-load conditions.

Finally a number of critical design points and potential issues have been discussed in this paper, which the designer is strongly recommended to remember during the design and development process and when working with real hardware in the laboratory.

References

- [1] Air Fuel Wireless Power Transfer System, Baseline System Specification (BSS), A4WP-S-0001 v1, Rezence, Alliance for Wireless Power.
- [2] Class-E RF Power Amplifiers, N.O. Sokal, QEX magazine #204 (American Radio Relay League)
- [3] Class-E High efficiency RF/microwave power amplifiers: Principles of operation, design procedures and experimental verification, N.O. Sokal
- [4] Idealized Operation of the Class-E tuned Power Amplifier, Frederick H. Raab MIEEE
- [5] Analytical Design Equations for Class-E Power Amplifiers, Mustafa Acar, Anne Johan Annema, Bram Nauta
- [6] Wireless Power Handbook, M.A. de Rooij, Efficient Power Corporation
- [7] Simple Inductance Formulas for Radio Coils (Proceedings of the I.R.E.), Harold A. Wheeler, October 1928
- [8] User manual of MCI's power receiving units, Management Center Innsbruck

Conclusion***Attention:***

Revision History

Major changes since the last revision

Page or Reference	Description of change
	First Release

Trademarks of Infineon Technologies AG

AURIX™, C166™, CanPAK™, CIPOST™, CoolGaN™, CoolMOS™, CoolSET™, CoolSiC™, CORECONTROL™, CROSSAVE™, DAVE™, DI-POL™, DrBlade™, EasyPIM™, EconoBRIDGE™, EconoDUAL™, EconoPACK™, EconoPIM™, EiceDRIVER™, eupec™, FCOST™, HITFET™, HybridPACK™, Infineon™, ISOFACE™, IsoPACK™, i-Wafer™, MIPAQ™, ModSTACK™, my-d™, NovalithIC™, OmniTune™, OPTIGA™, OptiMOS™, ORIGA™, POWERCODE™, PRIMARION™, PrimePACK™, PrimestACK™, PROFET™, PRO-SIL™, RASIC™, REAL3™, ReverSave™, SatRIC™, SIEGET™, SIPMOS™, SmartLEWIS™, SOLID FLASH™, SPOCT™, TEMPFET™, thinQ™, TRENCHSTOP™, TriCore™.

Trademarks updated August 2015

Other Trademarks

All referenced product or service names and trademarks are the property of their respective owners.

IMPORTANT NOTICE

The information contained in this application note is given as a hint for the implementation of the product only and shall in no event be regarded as a description or warranty of a certain functionality, condition or quality of the product. Before implementation of the product, the recipient of this application note must verify any function and other technical information given herein in the real application. Infineon Technologies hereby disclaims any and all warranties and liabilities of any kind (including without limitation warranties of non-infringement of intellectual property rights of any third party) with respect to any and all information given in this application note.

For further information on the product, technology, delivery terms and conditions and prices please contact your nearest Infineon Technologies office (www.infineon.com).

WARNINGS

Due to technical requirements products may contain dangerous substances. For information on the types in question please contact your nearest Infineon Technologies office.

Except as otherwise explicitly approved by Infineon Technologies in a written document signed by authorized representatives of Infineon Technologies, Infineon Technologies' products may not be used in any applications where a failure of the product or any consequences of the use thereof can reasonably be expected to result in personal injury.

**Edition 2018-01-25
Published by**

**Infineon Technologies AG
81726 Munich, Germany**

**© 2018 Infineon Technologies AG.
All Rights Reserved.**

**Do you have a question about this
document?**

Email: erratum@infineon.com

Document reference

AppNote Number

AN_2018-01-25-000

Trademarks of Infineon Technologies AG

AURIX™, C166™, CanPAK™, CIPOST™, CoolGaN™, CoolMOS™, CoolSET™, CoolSiC™, CORECONTROL™, CROSSAVE™, DAVE™, DI-POL™, DrBlade™, EasyPIM™, EconoBRIDGE™, EconoDUAL™, EconoPACK™, EconoPIM™, EiceDRIVER™, eupec™, FCOST™, HITFET™, HybridPACK™, Infineon™, ISOFACE™, IsoPACK™, i-Wafer™, MIPAQ™, ModSTACK™, my-d™, NovalithIC™, OmniTune™, OPTIGA™, OptiMOS™, ORIGA™, POWERCODE™, PRIMARION™, PrimePACK™, PrimestACK™, PROFET™, PRO-SIL™, RASIC™, REAL3™, ReverSave™, SatRIC™, SIEGET™, SIPMOS™, SmartLEWIS™, SOLID FLASH™, SPOCT™, TEMPFET™, thinQ™, TRENCHSTOP™, TriCore™.

Trademarks updated August 2015

Other Trademarks

All referenced product or service names and trademarks are the property of their respective owners.

IMPORTANT NOTICE

The information contained in this application note is given as a hint for the implementation of the product only and shall in no event be regarded as a description or warranty of a certain functionality, condition or quality of the product. Before implementation of the product, the recipient of this application note must verify any function and other technical information given herein in the real application. Infineon Technologies hereby disclaims any and all warranties and liabilities of any kind (including without limitation warranties of non-infringement of intellectual property rights of any third party) with respect to any and all information given in this application note.

For further information on the product, technology, delivery terms and conditions and prices please contact your nearest Infineon Technologies office (www.infineon.com).

WARNINGS

Due to technical requirements products may contain dangerous substances. For information on the types in question please contact your nearest Infineon Technologies office.

Except as otherwise explicitly approved by Infineon Technologies in a written document signed by authorized representatives of Infineon Technologies, Infineon Technologies' products may not be used in any applications where a failure of the product or any consequences of the use thereof can reasonably be expected to result in personal injury.

**Edition 2018-01-25
Published by**

**Infineon Technologies AG
81726 Munich, Germany**

**© 2018 Infineon Technologies AG.
All Rights Reserved.**

**Do you have a question about this
document?**

Email: erratum@infineon.com

**Document reference
AppNote Number**

AN_2018-01-25-001